ISME

Nonlinear Analysis of Flow-induced Vibration in Fluid-conveying Structures using Differential Transformation Method with Cosine-after Treatment Technique

Gbeminiyi M. Sobamowo *
Assistant Professor

In this work, analytical solutions are provided to the nonlinear equations arising in thermal and flow-induced vibration in fluid-conveying structures using Galerkin-differential transformation method with cosine aftertreatment technique. From the analysis, it was established that increase of the length and aspect ratio of the fluid-conveying structures result in decrease the nonlinear vibration frequencies of the structure while increase in the fluid-flow velocity causes increase in nonlinear vibration frequencies of the structures. Also, increase in the slip parameter leads to decrease in the frequency of vibration of the structure and the critical velocity of the conveyed fluid while increase in the slip parameter leads to decrease in the dimensionless frequency ratio of vibration of the structure. As the Knudsen number increases, the bending stiffness of the nanotube decreases and in consequent, the critical continuum flow velocity decreases as the curves shift to the lowest frequency zone. Good agreement are established when the results of the differential transformation method are compared with the results of the numerical method and exact analytical method for the non-linear and linear models, respectively.

Keyword: Non-linear Vibration; Galerkin's method; Differential Transformation method; Cosine-Aftertreatment techniques; Fluid-conveying structures.

1 Introduction

Flow-induced vibrations of fluid-conveying structures such as pipes, micro-pipes and nanotubes have been topics of wide research interests which have received numerous experimental, numerical, and theoretical studies over many past decades. Benjamin [1] studied dynamics of a system of articulated pipes conveying fluid. Housner et al. [2] investigated the effect of high velocity fluid flow in the bending vibration and static divergence of simply supported pipes while Holmes [3] submitted that pipe supported at both ends cannot flutter. Semler et al. [4] developed the non-linear equations of motion of pipes conveying fluid.

*Assistant Professor, Department of Mechanical Engineering, University of Lagos, Akoka, Lagos, Nigeria
mikegbeminiyi@gmail.com

Paidoussis [5] analyzed the dynamics behavior of flexible slender cylinders in axial flow while Paidoussis and Deksnis [6] presened articulated models of cantilevers conveying fluid. Rinaldi et al [7] stuied the stability of microscale pipes containing internal fluid flow while Akgoz and Civalek [8]presented vibration analysis of axially functionally graded tapered Bernoulli–Euler microbeams based on the modified couple stress theory. Xia and Wang [9] analyzed microfluid-induced vibration and stability of structures based on non-classical Timoshenko beam theory" while Ahangar et al. [10] used modified couple stress theory to analyze the stability of a microbeam conveying fluid considering. Yin et al [11] used strain gradient beam model for carry out the dynamics of microscale pipes conveying fluid. Sahmani et al. [12] adopted modified strain gradient elasticity theory nonlinear free vibration analysis of functionally graded third-order shear deformable microbeams.

Akgoz, and Civalek [13] presented buckling analysis of functionally graded microbeams based on the strain gradient theory Also, Zhao et al. [14] and Kong et al [15] applied strain gradient theory nonlinear dynamic behavior of microbeam model while Setoodeh and Afrahhim [16]studied nonlinear dynamic analysis of FG micro-pipes conveying fluid based on strain gradient theory. Yoon et al. [17] analyzed vibration and instability of carbon nanotubes conveying fluid. Yan et al [18] investigated the nonlocal effect on axially compressed buckling of triple-walled carbon nanotubes under temperature field. Murmu and Pradhan [19] studied thermo-mechanical vibration of Single-walled carbon nanotube embedded in an elastic medium based on nonlocal elasticity theory. Yang and Wang [20] presented bending stability of multi-wall carbon nanotubes embedded in an elastic medium. Yoon et al. [21] analyzed the vibration of an embedded multiwall carbon nanotube. Chang and Lee [22] used Timoshenko beam model to analyze vibration of a single-walled carbon nanotube containing a fluid flow. Lu et al. applied of nonlocal beam models for carbon nanotubes. Zhang et al. [23] studied transverse vibration of double-walled carbon nanotubes under compressive axial load. Ghorbanpour [24] analyzed the thermal effect on buckling analysis of a DWCNT embedded on the Pasternak foundation.

It is established from reviewed works that the dynamic analysis of flow-induced vibration in pipes, micropipes and nanotubes has become a subject of vast interests as it has attracted a large number of studies in literatures. This is because, modeling the dynamic behaviours of the structures under the influence of some thermo-fluidic or thermo-mechanical parameters often results in nonlinear equations and such are difficult to find the exact analytical solutions. In some cases where decomposition procedures into spatial and temporal parts are carried out, the resulting nonlinear equation for the temporal part comes in form of Duffing equation. Application of analytical methods such as Exp-function method, He's Exp-function method, improved F-expansion method, Lindstedt-Poincare techniques, quotient trigonometric function expansion method to the nonlinear equation present analytical solutions either in implicit or explicit form which often involved complex mathematical analysis leading to analytic expression involving a large number terms.

Furthermore, the methods are time-consuming task accompanied with possessing high skills in mathematics. Also, they do not provide general analytical solutions since the solutions often come with conditional statements which make them limited in used as many of the conditions with the exact solutions do not meet up with the practical applications.In practice, analytical solutions with large number of terms and conditional statements for the solutions are not convenient for use by designers and engineers [25].

Consequently, recourse has always been made to numerical methods or approximate analytical methods in solving the problems.However, the classical way for finding exact analytical solution is obviously still very important since it serves as an accurate benchmark for numerical solutions. Also, the experimental data are useful to access the mathematical models, but are never sufficient to verify the numerical solutions of the established mathematical models.

Comparison between the numerical calculations and experimental data often fail to reveal the compensation of modelling deficiencies through the computational errors or unconscious approximations in establishing applicable numerical schemes. Additionally, exact analytical solutions for specified problems are also essential for the development of efficient applied numerical simulation tools. Inevitably, exact analytical expressions are required to show the direct relationship between the models parameters.

When such exact analytical solutions are available, they provide good insights into the significance of various system parameters affecting the phenomena as it gives continuous physical insights than pure numerical or computation methods. Furthermore, most of the analytical approximation and purely numerical methods that were applied in literatures to nonlinear problems are computationally intensive. Exact analytical expression is more convenient for engineering calculations compare with experimental or numerical studies and it is obvious starting point for a better understanding of the relationship between physical quantities/properties. It is convenient for parametric studies, accounting for the physics of the problem and appears more appealing than the numerical solutions.

It appears more appealing than the numerical solution as it helps to reduce the computation costs, simulations and task in the analysis of real life problems. Therefore, an exact analytical solution is required for the problem.

Differential transform method is an approximate analytical method for solving differential equations Although, this concept was introduced by Zhou [26], its applications to both linear and non-linear differential and systems of differential equation have fast gained ground as it appeared in many engineering and scientific research papers. It is a method that could solve differential equations, difference equation, differential-difference equations, fractional differential equation, pantograph equation and integro-differential equation. It solves nonlinear integral and differential equations without linearization, discretization or restrictive assumptions, perturbation and discretization round-off error. Itreduces complexity of expansion of derivatives andthe computational difficulties of the other traditional methods.

Using DTM, a closed form series solution or approximate solution can be obtained as it provides excellent approximations to the solution of non-linear equation with high accuracy. It is capable of greatly reducing the size of computational work while still accurately providing the series solution with fast convergence rate. Also, DTM can be used to solve linear and non-linear non-homogeneous PDEs with accurate approximate, which is acceptable for small range. Laplace transform could be combined with the DTM to overcome the large range solution deficiency that is mainly caused by the unsatisfied conditions. DTM is more effective and convenient compared to the ADM and VIM. DTM does not require many computations as carried out in ADM and VIM to have high and fast rate of convergence.

Also, Galerkin's method provides a very powerful, novel and accurate approximate analytical solution procedure that is applicable to a wide variety of linear and non-linear problems. Combining the Galerkin's method with differential transform method in the analysis of non-linear initial-boundary value problems, provides complementary advantages of higher accuracy, reduced computation cost and task as compared to the other methods as found in literatures. Although, the hybrid method of Galerkin-differential transform method (GDTM) solves the differential equations without linearization, discretization or approximation, linearization restrictive assumptions or perturbation, complexity of expansion of derivatives and computation of derivatives symbolically, a well-known fact is that, the differential transformation method (DTM) gives the solution in the form of a truncated series. Unfortunately, in the case of oscillatory systems, the truncated series obtained by the method is periodic only in a very small region. This drawback is not only peculiar to DTM, other approximate analytical methods such as ADM also have the same short-coming for oscillatory systems [27, 28].

To overcome this difficulty, an aftertreatment technique (AT) was used to obtain approximate periodic solutions in a wide range of solution. In modifying ADM to provide periodic solutions in a large region, Venkatarangan and Rajakshmi [27] and Jiao *et al.* [28] developed AT techniques which are based onusing Pade approximates, Laplace transform and its inverse. Although, the AT techniques were found to be effective in many cases, it has some disadvantages, not only it required a huge amountof computational work to provide accurate approximations for the periodic solutions but also thereis a difficulty of obtaining the inverse Laplace transform which greatly restricts the application areaof their technique [29]. In this work, the after treatment techniqueas developed by Elhalim and Emad [29] which has shown to be better than previously developed aftertreatment techniques is applied. Therefore, in this research, analytical solutions are provided to the nonlinear partial differential equations arising in flow-induced vibration in pipes, micro-pipes and nanotubesunder different boundary conditions using Galerkin-differential transformation method with aftertreatment technique.
The nonlinear partial differential equations were converted to nonlinear ordinary differential equations and then differential transformation method with after treatment technique is utilized to provide exact analytical solutions to the nonlinear ordinary differential equations of vibration of the structures. The developed analytical solutions are compared with the numerical results and the results of approximate analytical solutions and good agreements reached. The analytical solutions can serve as a starting point for a better understanding of the relationship between the physical quantities of the problems as it provides continuous physical insights into the problem than pure numerical or computation methods.

2 Governing equations and boundary conditions

Case 1: Flow-induced vibration in pipe

Consider a pipe conveying hot fluid, subjected to stretching effects and resting on linear and nonlinear elastic foundations (Pasternak, linear and nonlinear Winkler foundations) under external applied tension and global pressure as shown in Figure (1). Using nonlocal elasticity theory and Hamilton's principle, the governing equation of motion for the is given as

$$EI\frac{\partial^4 w}{\partial x^4}+(m_p+m_f)\frac{\partial^2 w}{\partial t^2}+\mu\frac{\partial w}{\partial t}+2vm_f\frac{\partial^2 w}{\partial x\partial t}+\left(m_f v^2+PA-T-k_p-\frac{EA\alpha\Delta\theta}{1-2\nu}\right)\frac{\partial^2 w}{\partial x^2}$$
$$+k_1 w+k_3 w^3-\left[N_o+\frac{EA}{2L}\int_0^L\left(\frac{\partial w}{\partial x}\right)^2 dx\right]\frac{\partial^2 w}{\partial x^2}=0 \quad (1)$$

If the pipe is slightly curved, then the governing equation becomes

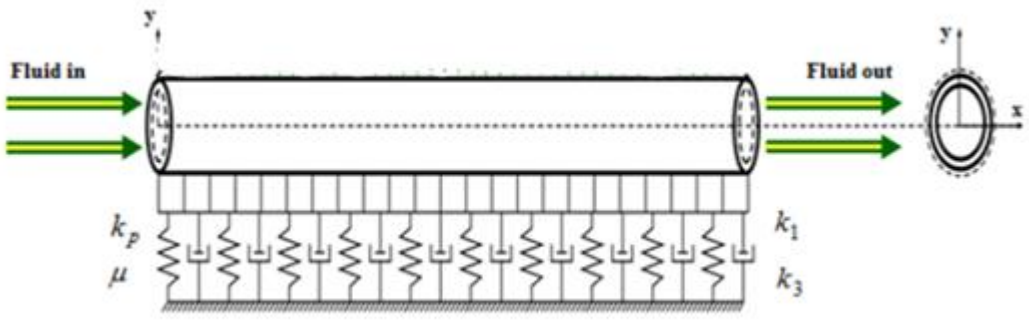

Figure 1 Geometry and loading of the problem

$$EI\frac{\partial^4 w}{\partial x^4}+(m_p+m_f)\frac{\partial^2 w}{\partial t^2}+\mu\frac{\partial w}{\partial t}+2vm_f\frac{\partial^2 w}{\partial x\partial t}+\left(m_f v^2+PA-T-k_p-\frac{EA\alpha\Delta\theta}{1-2\nu}\right)\frac{\partial^2 w}{\partial x^2}$$
$$+k_1 w+k_3 w^3-\left[N_o+\frac{EA}{2L}\int_0^L\left\{\frac{\partial Z_o}{\partial x}\frac{\partial w}{\partial x}+\left(\frac{\partial w}{\partial x}\right)^2\right\}dx\right]\left[\frac{\partial^2 w}{\partial x^2}+\frac{\partial^2 Z_o}{\partial x^2}\right]=0 \quad (2)$$

Where $Z_o(x)$ is the arbitrary initial rise function.
Using the Galerkin's decomposition procedure to separate the spatial and temporal parts of the lateral displacement functions as

$$w(x,t)=\phi(x)u(t) \quad (3)$$

Where $u(t)$ the generalized coordinate of the system and $\phi(x)$ is a trial/comparison function that will satisfy both the geometric and natural boundary conditions.
Applying one-parameter Galerkin's solution given in Eq. (4) to Eq. (3)

$$\int_0^L R(x,t)\phi(x)dx \quad (4)$$

Where for the straight pipe

$$R(x,t)=EI\frac{\partial^4 w}{\partial x^4}+(m_p+m_f)\frac{\partial^2 w}{\partial t^2}+\mu\frac{\partial w}{\partial t}+2vm_f\frac{\partial^2 w}{\partial x\partial t}+\left(m_f v^2+PA-T-k_p-\frac{EA\alpha\Delta\theta}{1-2\nu}\right)\frac{\partial^2 w}{\partial x^2}$$
$$+k_1 w+k_3 w^3-\left[N_o+\frac{EA}{2L}\int_0^L\left(\frac{\partial w}{\partial x}\right)^2 dx\right]\frac{\partial^2 w}{\partial x^2}=0$$

And for the slightly curved pipe

$$R(x,t)=EI\frac{\partial^4 w}{\partial x^4}+(m_p+m_f)\frac{\partial^2 w}{\partial t^2}+\mu\frac{\partial w}{\partial t}+2vm_f\frac{\partial^2 w}{\partial x\partial t}+\left(m_f v^2+PA-T-k_p-\frac{EA\alpha\Delta\theta}{1-2\nu}\right)\frac{\partial^2 w}{\partial x^2}$$
$$+k_1 w+k_3 w^3-\left[N_o+\frac{EA}{2L}\int_0^L\left\{\frac{\partial Z_o}{\partial x}\frac{\partial w}{\partial x}+\left(\frac{\partial w}{\partial x}\right)^2\right\}dx\right]\left[\frac{\partial^2 w}{\partial x^2}+\frac{\partial^2 Z_o}{\partial x^2}\right]=0$$

We have the nonlinear vibration equation of the pipe as

$$M\ddot{u}(t)+G\dot{u}(t)+(K+C)u(t)-Vu^3(t)=0 \quad (5)$$

Where

$$M=\int_0^L(m_p+m_f)\phi^2(x)dx$$

$$G=\int_0^L\left[2m_f u\phi(x)\left(\frac{d\phi}{dx}\right)+\mu\phi^2(x)\right]dx$$

$$K=\int_0^L\left[EI\phi(x)\frac{d^4\phi}{dx^4}+k_1\phi^2(x)+k_p\phi(x)\frac{d^2\phi}{dx^2}\right]dx$$

$$C=\int_0^L\left(m_f u^2+PA-T-\frac{EA\alpha\Delta\theta}{1-2\nu}\right)\phi(x)\frac{d^2\phi}{dx^2}\,dx$$

$$V=\int_0^L\left\{\phi(x)\left[N_o+\frac{EA}{2L}\int_0^L\left(\frac{\partial w}{\partial x}\right)^2dx\right]\frac{d^2\phi}{dx^2}-k_3\phi^3(x)\right\}dx$$

For the slightly curved pipe, *M*, *G*, *K* and *C* are the same but

$$V=\int_0^L\left\{\phi(x)\left[N_o+\frac{EA}{2L}\int_0^L\left\{\frac{\partial Z_o}{\partial x}\frac{\partial w}{\partial x}+\left(\frac{\partial w}{\partial x}\right)^2\right\}dx\right]\left[\frac{\partial^2 w}{\partial x^2}+\frac{\partial^2 Z_o}{\partial x^2}\right]-k_3\phi^3(x)\right\}dx$$

The circular fundamental natural frequency gives

$$\omega_n=\sqrt{\frac{K+C^*}{M}}\qquad(6)$$

$$C^*=\int_0^L\left(PA-T-\frac{EA\alpha\Delta\theta}{1-2\nu}\right)\phi(x)\frac{d^2\phi}{dx^2}\,dx$$

Case 2: Flow induced vibration in functionally graded micro-pipe

Consider the case of flow induced vibration in a functionally graded micropipe conveying hot fluid subjected to stretching effects and resting on linear and nonlinear elastic foundation under external applied tension and global pressure. Applying strain gradient and coupled stress theories followed by Hamilton's principle [16], we arrived at the governing equation of motion for the functionally graded micropipe is given as

$$\left[GA_{eq}\left(2l_o^2+\frac{4}{5}l_1^2\right)\right]\frac{\partial^6 w}{\partial x^6}+\left[EI+GA_{eq}\left(2l_o^2+\frac{8}{15}l_1+l_1^2\right)\right]\frac{\partial^4 w}{\partial x^4}+(m_p+m_f)\frac{\partial^2 w}{\partial t^2}+\mu\frac{\partial w}{\partial t}+2vm_f\frac{\partial^2 w}{\partial x\partial t}$$
$$+\left(m_f v^2+PA-T-k_p-\frac{EA\alpha\Delta\theta}{1-2\nu}\right)\frac{\partial^2 w}{\partial x^2}+k_1 w+k_3 w^3-\left[N_o+\frac{EA}{2L}\int_0^L\left(\frac{\partial w}{\partial x}\right)^2dx\right]\frac{\partial^2 w}{\partial x^2}=0\qquad(7)$$

If the pipe is slightly curved, then the governing equation for the FG micropipe becomes

$$\left[GI_{eq}\left(2l_o^2+\frac{4}{5}l_1^2\right)\right]\frac{\partial^6 w}{\partial x^6}+\left[EI_{eq}+GA_{eq}\left(2l_o^2+\frac{8}{15}l_1+l_1^2\right)\right]\frac{\partial^4 w}{\partial x^4}+(m_p+m_f)\frac{\partial^2 w}{\partial t^2}+\mu\frac{\partial w}{\partial t}+2vm_f\frac{\partial^2 w}{\partial x\partial t}$$
$$+\left(m_f v^2+PA-T-k_p-\frac{EA_{eq}\alpha\Delta\theta}{1-2\nu}\right)\frac{\partial^2 w}{\partial x^2}+k_1 w+k_3 w^3-\left[N_o+\frac{EA_{eq}}{2L}\int_0^L\left\{\frac{\partial Z_o}{\partial x}\frac{\partial w}{\partial x}+\left(\frac{\partial w}{\partial x}\right)^2\right\}dx\right]\left[\frac{\partial^2 w}{\partial x^2}+\frac{\partial^2 Z_o}{\partial x^2}\right]=0\qquad(8)$$

Where

$$EI_{eq} = \int_A E(r)z^2 dA = \int_0^{2\pi} \int_{r_i}^{r_o} E(r)r^2 sin^2(\theta)(rdrd\theta)$$

$$GI_{eq} = \int_A G(r)z^2 dA = \int_0^{2\pi} \int_{r_i}^{r_o} EG(r)r^2 sin^2(\theta)(rdrd\theta)$$

$$EA_{eq} = \int_A E(r)dA = \int_0^{2\pi} \int_{r_i}^{r_o} E(r)(rdrd\theta)$$

$$GA_{eq} = \int_A G(r)dA = \int_0^{2\pi} \int_{r_i}^{r_o} G(r)(rdrd\theta)$$

$$E(r) = \left(\frac{r_o - r}{r_o - r_i}\right)^n E^i + \left[1 - \left(\frac{r_o - r}{r_o - r_i}\right)^n\right] E^o$$

$$\mathrm{G}(r) = \left(\frac{r_o - r}{r_o - r_i}\right)^n G^i + \left[1 - \left(\frac{r_o - r}{r_o - r_i}\right)^n\right] G^o$$

$$\alpha(r) = \left(\frac{r_o - r}{r_o - r_i}\right)^n \alpha^i + \left[1 - \left(\frac{r_o - r}{r_o - r_i}\right)^n\right] \alpha^o$$

$$m_p = \rho A$$

and

$$\rho(r) = \left(\frac{r_o - r}{r_o - r_i}\right)^n \rho^i + \left[1 - \left(\frac{r_o - r}{r_o - r_i}\right)^n\right] \rho^o$$

l_o, l_1 and $l_2$are the independent length scale parameters embedded in the constitutive equations of the higher order stresses.

If we follow the same procedure of applying the Galerkin's decomposition procedure to separate the spatial and temporal parts of the lateral displacement and then apply the one-parameter Galerkin's solution, we arrived at the same nonlinear vibration equation for the micropipe as

$$M\ddot{u}(t) + G\dot{u}(t) + (K + C)u(t) - Vu^3(t) = 0 \tag{9}$$

But at this time, we have

$$M = \int_0^L (m_p + m_f)\phi^2(x)dx$$

$$G = \int_0^L \left[2m_f u\phi(x)\left(\frac{d\phi}{dx}\right) + \mu\phi^2(x)\right]dx$$

$$K=\int_0^L\left\{\left[EI+GA_{eq}\left(2l_o^2+\frac{8}{15}l_1+l_1^2\right)\right]\phi(x)\frac{d^4\phi}{dx^4}+\left[GA_{eq}\left(2l_o^2+\frac{4}{5}l_1^2\right)\right]\frac{\partial^6\phi}{\partial x^6}+k_1\phi^2(x)+k_p\phi(x)\frac{d^2\phi}{dx^2}\right\}dx$$

$$C=\int_0^L\left(m_f u^2+PA-T-\frac{EA\alpha\Delta\theta}{1-2\nu}\right)\phi(x)\frac{d^2\phi}{dx^2}dx$$

$$V=\int_0^L\phi(x)\left\{\left[N_o+\frac{EA}{2L}\int_0^L\left(\frac{\partial\phi}{\partial x}\right)^2dx\right]\frac{d^2\phi}{dx^2}-k_3\frac{d^3\phi}{dx^3}\right\}dx$$

For the slightly curved FG micropipe, *M*, *G*, *K* and *C* are the same but

$$V=\int_0^L\phi(x)\left\{\left[N_o+\frac{EA}{2L}\int_0^L\left\{\frac{\partial Z_o}{\partial x}\frac{\partial w}{\partial x}+\left(\frac{\partial w}{\partial x}\right)^2\right\}dx\right]\left[\frac{\partial^2 w}{\partial x^2}+\frac{\partial^2 Z_o}{\partial x^2}\right]-k_3\frac{d^3\phi}{dx^3}\right\}dx$$

The circular fundamental natural frequency gives

$$\omega_n=\sqrt{\frac{K+C^*}{M}} \tag{10}$$

Where

$$C^*=\int_0^L\left(PA-T-\frac{EA\alpha\Delta\theta}{1-2\nu}\right)\phi(x)\frac{d^2\phi}{dx^2}dx$$

Case 3: Flow-induced vibration in nanotube

Consider a single-walled carbon nanotube conveying hot fluid, subjected to stretching effectsand resting on linear and nonlinear elastic foundation under external applied tension and global pressure. Following the Eringen's nonlocal elasticity theory [30-33] and Hamilton's principle, we arrived at the governing equation of motion for the single-walled carbon nanotube (SWCBT) as

$$EI\frac{\partial^4 w}{\partial x^4}+(m_p+m_f)\frac{\partial^2 w}{\partial t^2}+\mu\frac{\partial w}{\partial t}+2vm_f\frac{\partial^2 w}{\partial x\partial t}+\left(m_f v^2+PA-T-k_p-\frac{EA\alpha\Delta\theta}{1-2\nu}\right)\frac{\partial^2 w}{\partial x^2}-\left[\frac{EA}{2L}\int_0^L\left(\frac{\partial w}{\partial x}\right)^2dx\right]\frac{\partial^2 w}{\partial x^2}$$
$$+k_1w+k_3w^3-\left(e_o a\right)^2\left[\begin{array}{l}(m_p+m_f)\dfrac{\partial^4 w}{\partial x^2\partial t^2}+\mu\dfrac{\partial^3 w}{\partial x^2\partial t}+k_1\dfrac{\partial^2 w}{\partial x^2}+6k_3w\left(\dfrac{\partial w}{\partial x}\right)^2+3w^2\dfrac{\partial w}{\partial x}+2vm_f\dfrac{\partial^4 w}{\partial x^3\partial t}\\+\left(m_f v^2+PA-T-k_p-\dfrac{EA\alpha\Delta\theta}{1-2\nu}\right)\dfrac{\partial^4 w}{\partial x^4}-\left[\dfrac{EA}{2L}\int_0^L\left(\dfrac{\partial w}{\partial x}\right)^2dx\right]\dfrac{\partial^4 w}{\partial x^4}\end{array}\right]=0$$

(11)

If the nanotube is slightly curved, then the governing equation for the nanotube becomes

$$EI\frac{\partial^4 w}{\partial x^4}+(m_p+m_f)\frac{\partial^2 w}{\partial t^2}+\mu\frac{\partial w}{\partial t}+2vm_f\frac{\partial^2 w}{\partial x\partial t}+\left(m_f v^2+PA-T-k_p-\frac{EA\alpha\Delta\theta}{1-2\nu}\right)\frac{\partial^2 w}{\partial x^2}$$
$$-\left[N_o+\frac{EA}{2L}\int_0^L\left\{\frac{\partial Z_o}{\partial x}\frac{\partial w}{\partial x}+\left(\frac{\partial w}{\partial x}\right)^2\right\}dx\right]\left[\frac{\partial^2 w}{\partial x^2}+\frac{\partial^2 Z_o}{\partial x^2}\right]+k_1 w+k_3 w^3$$
$$-(e_o a)^2\left[\begin{array}{l}(m_p+m_f)\frac{\partial^4 w}{\partial x^2\partial t^2}+\mu\frac{\partial^3 w}{\partial x^2\partial t}+k_1\frac{\partial^2 w}{\partial x^2}+6k_3 w\left(\frac{\partial w}{\partial x}\right)^2+3w^2\frac{\partial w}{\partial x}+2vm_f\frac{\partial^4 w}{\partial x^3\partial t}\\+\left(m_f v^2+PA-T-k_p-\frac{EA\alpha\Delta\theta}{1-2\nu}\right)\frac{\partial^4 w}{\partial x^4}-\left[N_o+\frac{EA}{2L}\int_0^L\left\{\frac{\partial Z_o}{\partial x}\frac{\partial w}{\partial x}+\left(\frac{\partial w}{\partial x}\right)^2\right\}dx\right]\left[\frac{\partial^4 w}{\partial x^4}+\frac{\partial^4 Z_o}{\partial x^4}\right]\end{array}\right]=0 \quad (12)$$

For nanotube conveying fluid, the radius of the tube is assumed to be the characteristics length scale, Knudsen number is larger than 10^{-2}. Therefore, the assumption of no-slip boundary conditions does not hold and modified model should be used. Therefore, we have

$$VCF=\frac{U_{avg,slip}}{U_{avg,no-slip}}=(1+a_k Kn)\left[4\left(\frac{2-\sigma_v}{\sigma_v}\right)\left(\frac{Kn}{1+Kn}\right)+1\right] \quad (13)$$

Where *Kn* is the Knudsen number, $\sigma_v$is tangential moment accommodation coefficient which is considered to be 0.7 for most practical purposes [34].

$$a_k=a_o\frac{2}{\pi}\left[tan^{-1}\left(a_1 Kn^B\right)\right] \quad (14)$$

$$a_o=\frac{64}{3\pi\left(1-\frac{4}{b}\right)} \quad (15)$$

Therefore,

$$U_{avg,slip}=(1+a_k Kn)\left[4\left(\frac{2-\sigma_v}{\sigma_v}\right)\left(\frac{Kn}{1+Kn}\right)+1\right]U_{avg,no-slip}=VCF\left(U_{avg,no-slip}\right) \quad (16)$$

And Eq. (12) could be written as

$$EI\frac{\partial^4 w}{\partial x^4}+(m_p+m_f)\frac{\partial^2 w}{\partial t^2}+\mu\frac{\partial w}{\partial t}+2m_f\left[VCF\left(U_{avg,no-slip}\right)\right]\frac{\partial^2 w}{\partial x\partial t}+\left(m_f\left[VCF\left(U_{avg,no-slip}\right)\right]^2+PA-T-k_p-\frac{EA\alpha\Delta\theta}{1-2\nu}\right)\frac{\partial^2 w}{\partial x^2}$$
$$-\left[N_o+\frac{EA}{2L}\int_0^L\left\{\frac{\partial Z_o}{\partial x}\frac{\partial w}{\partial x}+\left(\frac{\partial w}{\partial x}\right)^2\right\}dx\right]\left[\frac{\partial^2 w}{\partial x^2}+\frac{\partial^2 Z_o}{\partial x^2}\right]+k_1 w+k_3 w^3$$
$$-(e_o a)^2\left[\begin{array}{l}(m_p+m_f)\frac{\partial^4 w}{\partial x^2\partial t^2}+\mu\frac{\partial^3 w}{\partial x^2\partial t}+k_1\frac{\partial^2 w}{\partial x^2}+6k_3 w\left(\frac{\partial w}{\partial x}\right)^2+3w^2\frac{\partial w}{\partial x}+2m_f\left[VCF\left(U_{avg,no-slip}\right)\right]\frac{\partial^4 w}{\partial x^3\partial t}\\+\left(m_f\left[VCF\left(U_{avg,no-slip}\right)\right]^2+PA-T-k_p-\frac{EA\alpha\Delta\theta}{1-2\nu}\right)\frac{\partial^4 w}{\partial x^4}-\left[N_o+\frac{EA}{2L}\int_0^L\left\{\frac{\partial Z_o}{\partial x}\frac{\partial w}{\partial x}+\left(\frac{\partial w}{\partial x}\right)^2\right\}dx\right]\left[\frac{\partial^4 w}{\partial x^4}+\frac{\partial^4 Z_o}{\partial x^4}\right]\end{array}\right]=0 \quad (17)$$

Again, following the same procedure of applying the Galerkin's decomposition procedure and then apply the one-parameter Galerkin's solution, we arrived at the same nonlinear vibration equation for the nanotube as

$$M\ddot{u}(t)+G\dot{u}(t)+(K+C)u(t)-Vu^3(t)=0 \tag{18}$$

Here, we have

$$M=\int_0^L (m_p+m_f)\phi(x)\left(\phi(x)-(e_oa)^2\frac{d^2\phi}{dx^2}\right)+\phi(x)\left(m_fu^2\phi(x)-(e_oa)^2\frac{d^2\phi}{dx^2}\right)dx$$

$$G=\int_0^L \phi(x)\left\{\left(2m_fv\frac{d\phi}{dx}-(e_oa)^2\frac{d^3\phi}{dx^3}\right)+\left(\mu\phi(x)-(e_oa)^2\frac{d^2\phi}{dx^2}\right)\right\}dx$$

$$K=\int_0^L \phi(x)\left\{EI\frac{d^4\phi}{dx^4}+k_1\phi(x)-k_p\frac{d^2\phi}{dx^2}-k_1\left(e_oa\right)^2\frac{d^2\phi}{dx^2}+\left(e_oa\right)^2k_p\frac{d^2\phi}{dx^2}\right\}dx$$

$$C=\int_0^L\left(m_fu^2+PA-T-\frac{EA\alpha\Delta\theta}{1-2\nu}\right)\phi(x)\left(\frac{d^2\phi}{dx^2}-(e_oa)^2\frac{d^4\phi}{dx^4}\right)dx$$

$$V=\int_0^L\phi(x)\begin{Bmatrix}\left[N_o+\dfrac{EA}{2L}\int_0^L\left(\dfrac{\partial\phi}{\partial x}\right)^2dx\right]\dfrac{d^2\phi}{dx^2}-k_3\dfrac{d^3\phi}{dx^3}(x)+6k_3(e_oa)^2\phi(x)\left(\dfrac{\partial\phi}{\partial x}\right)^2\\ -3k_3(e_oa)^2\phi^2(x)\dfrac{\partial\phi}{\partial x}-(e_oa)^2\left[N_o+\dfrac{EA}{2L}\int_0^L\left(\dfrac{\partial\phi}{\partial x}\right)^2dx\right]\dfrac{d^4\phi}{dx^4}\end{Bmatrix}dx$$

For the slightly curved nanotube, *M*, *G*, *K* and *C* are the same but

$$V=\int_0^L\phi(x)\begin{Bmatrix}\left[N_o+\dfrac{EA}{2L}\int_0^L\left\{\dfrac{\partial Z_o}{\partial x}\dfrac{\partial w}{\partial x}+\left(\dfrac{\partial w}{\partial x}\right)^2\right\}dx\right]\left[\dfrac{\partial^2w}{\partial x^2}+\dfrac{\partial^2Z_o}{\partial x^2}\right]-k_3\dfrac{d^3\phi}{dx^3}(x)+6k_3(e_oa)^2\phi(x)\left(\dfrac{\partial\phi}{\partial x}\right)^2\\ -3k_3(e_oa)^2\phi^2(x)\dfrac{\partial\phi}{\partial x}-(e_oa)^2\left[N_o+\dfrac{EA}{2L}\int_0^L\left\{\dfrac{\partial Z_o}{\partial x}\dfrac{\partial w}{\partial x}+\left(\dfrac{\partial w}{\partial x}\right)^2\right\}dx\right]\left[\dfrac{\partial^4w}{\partial x^4}+\dfrac{\partial^4Z_o}{\partial x^4}\right]\end{Bmatrix}dx$$

and the circular fundamental natural frequency gives

$$\omega_n=\sqrt{\frac{K+C^*}{M}} \tag{19}$$

Where

$$C^*=\int_0^L\left(PA-T-\frac{EA\alpha\Delta\theta}{1-2\nu}\right)\phi(x)\left(\frac{d^2\phi}{dx^2}-(e_oa)^2\frac{d^4\phi}{dx^4}\right)dx$$

3 The initial and boundary conditions

The structures (pipe, micopipe and nanotube) may be subjected to any of the following boundary conditions

i. Clamped-Clamped (doubly clamped)

Where the trial/comparison function are given as

$$\phi(x) = cosh\beta_n x - cos\beta_n x - \left(\frac{cosh\beta_n L - cos\beta_n L}{sinh\beta_n L - sin\beta_n L}\right)\left(sinh\beta_n x - sin\beta_n x\right) \tag{20}$$

or

$$\phi(x) = cosh\beta_n x - cos\beta_n x - \left(\frac{sinh\beta_n L + sin\beta_n L}{cosh\beta_n L - cos\beta_n L}\right)\left(sinh\beta_n x - sin\beta_n x\right) \tag{21}$$

Where β_n are the roots of the equation

$$cos\beta_n L cosh\beta_n L = 1$$

The initial and the boundary conditions are

$$\begin{gathered} w(0,x) = A \;\; \dot{w}(0,x) = 0 \\ w(0,t) = w'(0,t) = 0 \;\; w(L,t) = w'(L,t) = 0 \end{gathered} \tag{22}$$

The applications of space function as given above for clamped-clamped will involve long calculations and expressions in Finding *M, G, K, C,* and *V*, alternatively, a polynomial function of the form Eq. (23) can be applied for this type of support system.

$$\phi(x) = a_o + a_1 X + a_2 X^2 + a_3 X^3 + a_4 X^4 \tag{23}$$

Where $X = \frac{x}{L}$

Applying the boundary conditions

$$\phi(x) = \left(X^2 - 2X^3 + X^4\right) a_4 \tag{24}$$

Orthogonal function should satisfy the equation

$$\int_0^a \phi(X)\phi(X)dx = 1 \tag{25}$$

Substitute Eq. (24) into Eq. (25), we have

$$a_4 = 3\sqrt{70}\left(\sqrt{\frac{1}{a^5\left(70a^4 - 315a^3 + 540a^2 - 420a + 126\right)}}\right) \tag{26}$$

For a=1, arrived at $a_4 = 25.20$ for the first mode

ii. Clamped-Simple supported

The trial/comparison function are given as

$$\phi(x) = cosh\beta_n x - cos\beta_n x - \left(\frac{cosh\beta_n L - cos\beta_n L}{sinh\beta_n L - sin\beta_n L}\right)\left(sinh\beta_n x - sin\beta_n x\right) \tag{27}$$

β_n are the roots of the equation

$$tan\beta_n L = tanh\beta_n L$$

The initial and the boundary conditions are

$$w(0,x) = A \;\; \dot{w}(0,x) = 0$$
$$w(0,t) = w'(0,t) = 0 \;\; w(L,t) = w''(L,t) = 0 \tag{28}$$

Alternatively, a polynomial function of the form Eq. (29) can be applied for this type of support system.

$$\phi(x) = \left(\frac{3}{2}X^2 - \frac{5}{2}X^3 + X^4\right)a_4 \tag{29}$$

On using orthogonal functions, $a_4 = 11.625$ for the first mode

iii. Simple-Simple supported

$$\phi(x) = sin\beta_n x \tag{30}$$
$$sin\beta L = 0 \quad \Rightarrow \beta_n = \frac{n\pi}{L}$$

The initial and the boundary conditions are

$$w(0,x) = A \;\; \dot{w}(0,x) = 0$$
$$w(0,t) = w''(0,t) = 0 \;\; w(L,t) = w''(L,t) = 0 \tag{31}$$

Alternatively, a polynomial function of the form Eq. (31) can be applied for this type of support system.

$$\phi(x) = \left(X - 2X^3 + X^4\right)a_4 \tag{32}$$

On using orthogonal functions, $a_4 = 3.20$ for the first mode

iv. Clamp-Free (cantilever)

$$\phi(x) = cosh\beta_n x - cos\beta_n x - \left(\frac{cosh\beta_n L + cos\beta_n L}{sinh\beta_n L + sin\beta_n L}\right)\left(sinh\beta_n x - sin\beta_n x\right) \tag{33}$$

or

$$\phi(x) = cosh\beta_n x - cos\beta_n x - \left(\frac{sinh\beta_n L - sin\beta_n L}{cosh\beta_n L - cos\beta_n L}\right)\left(sinh\beta_n x - sin\beta_n x\right) \tag{34}$$

β_n are the roots of the equation

$$cos\beta_n L cosh\beta_n L = -1$$

The initial and the boundary conditions are

$$w(0,x)=A\ \dot{w}(0,x)=0$$
$$w(0,t)=w'(0,t)=0\ w''(L,t)=w'''(L,t)=0 \tag{35}$$

Alternatively, a polynomial function of the form Eq. (36) can be applied for this type of support system.

$$\phi(x)=\left(6X^2-4X^3+X^4\right)a_4 \tag{36}$$

Also, with the aid of orthogonal functions, $a_4=0.6625$ for the first mode

4 Determination of natural frequencies

The natural frequency analysis is the sine qua non for the analysis of stability, it must therefore be carried out in the dynamic response of the structures.

Under the transformation, $\tau=\omega t$, Eq. (5) turns out to be

$$M\omega^2\ddot{u}(\tau)+G\omega\dot{u}(\tau)+(K+C)u(\tau)-Vu^3(\tau)=0 \tag{37}$$

For the undamped clamped-clamped, clamped-simple and simple-simple supported structures, *G=0*

$$M\omega^2\ddot{u}(\tau)+(K+C)u(\tau)-Vu^3(\tau)=0 \tag{38}$$

In order to find the periodic solution of Eq. (38), assume an initial approximation for zero-order deformation to be

$$u_o(\tau)=A\cos\tau \tag{39}$$

$$-M\omega_o^2A\cos\tau+(K+C)A\cos\tau-VA^3\cos^3\tau=0 \tag{40}$$

$$-M\omega^2A\cos\tau+(K+C)A\cos\tau-VA^3\left(\frac{3\cos\tau+\cos3\tau}{4}\right)=0$$

$$\left((K+C)A-\frac{3VA^3}{4}-M\omega^2A\right)\cos\tau-\frac{1}{4}VA^3\cos3\tau=0 \tag{41}$$

In order to eliminate the secular term, we have

$$\left((K+C)A-\frac{3VA^3}{4}-M\omega_o^2A\right)=0 \tag{42}$$

Thus, for the zero-order nonlinear natural frequency, we have

$$\omega_o\approx\sqrt{\frac{K+C}{M}-\frac{3VA^2}{4M}} \tag{43}$$

Therefore, the ratio of the zero-order nonlinear natural frequency, ω_o to the linear frequency, ω_b

$$\frac{\omega_o}{\omega_b} \approx \sqrt{1-\frac{3VA^2}{4(K+C)}} \tag{44}$$

Similarly, for the first-order nonlinear natural frequency, we have

$$\omega_1 \approx \sqrt{\frac{1}{2}\left\{\left[\left(\frac{K+C}{M}\right)-\left(\frac{3VA^2}{4M}\right)\right]+\sqrt{\left[\left(\frac{K+C}{M}\right)-\left(\frac{3VA^2}{4M}\right)\right]^2-\left(\frac{3V^2A^4}{32M^2}\right)}\right\}} \tag{45}$$

The ratio of thefirst-order nonlinear frequency, ω_1 to the linear frequency, ω_b

$$\frac{\omega_1}{\omega_b} \approx \sqrt{\frac{1}{2}\left\{\left[1-\left(\frac{3VA^2}{4(K+C)}\right)\right]+\sqrt{\left[1-\left(\frac{3VA^2}{4(K+C)}\right)\right]^2-\left(\frac{3V^2A^4}{32(K+C)}\right)}\right\}} \tag{46}$$

On a general note, following Lai *et al.* [67], it can easily be shown that the exact natural frequency of the fluid-conveying structures is given as

$$\omega_{1,exact} = \frac{\pi\xi_1}{2\left[\int_0^{\pi/2}\left(1+\xi_2 sin^2 t\right)^{-\frac{1}{2}}dt\right]} \tag{47}$$

For the general case in this work,

$$\xi_1 = \left[\left(\frac{K+C}{M}\right)-\left(\frac{VA^2}{2M}\right)\right]^{\frac{1}{2}} \quad \xi_2 = \frac{\left(\frac{VA^2}{M}\right)}{\left[\left(\frac{VA^2}{M}\right)-2\left(\frac{K+C}{M}\right)\right]}$$

Where when the nonlinear term, V is set to zero, we recovered the linear natural frequency.

It is very difficult to generate exact solution of Eq. (47), using series integration method, we developed an approximation analytical solution for finding the natural frequency as

$$\omega_1 \approx \xi_1\left[1-0.25000\xi_2+0.11680{\xi_2}^2-0.59601{\xi_2}^3-1.90478{\xi_2}^4-2.04574{\xi_2}^5\right] \tag{48}$$

The ratio of the first-order nonlinear frequency, ω_1 to the linear frequency, ω_b

$$\frac{\omega_1}{\omega_b} \approx \left[1-0.25000\xi_2+0.11680{\xi_2}^2-0.59601{\xi_2}^3-1.90478{\xi_2}^4-2.04574{\xi_2}^5\right] \tag{49}$$

Also, it is difficult to generate any closed form solution for the above nonlinear Eq. (5 or 9 or 18). In finding simple, direct and practical solutions to the problem, we apply differential transformation with after treatment technique to the nonlinear equation.

5 Differential transformation method

As pointed previously, the differential transformation method is an approximate analytical method for solving differential equations. However, a closed form series solution or approximate solution can be obtained for non-linear differential equations with the use of DTM. The basic definitions of the method is as follows
If $u(t)$ is analytic in the domain T, then it will be differentiated continuously with respect to time *t*.

$$\frac{d^K u(t)}{dt^K} = \phi(t,k) \text{ for } \quad \text{all } t \in T \tag{50}$$

for $t = t_i$, then $\phi(t,k) = \phi(t_i, K)$, where K belongs to the set of non-negative integers, denoted as the K-domain. Therefore Eq. (50) can be rewritten as

$$U(k) = \phi(t_i, k) = \left[\frac{d^k u(t)}{dt^K}\right]_{t=t_i} \tag{51}$$

Where U_k is called the spectrum of $u(t)$ at $t = t_i$

If $u(t)$ can be expressed by Taylor's series, the $u(t)$ can be represented as

$$u(t) = \sum_k^{\infty}\left[\frac{(t-t_i)^K}{k!}\right] U(k) \tag{52}$$

Where Equ. (52) is called the inverse of $U(k)$ using the symbol 'D' denoting the differential transformation process and combining (51) and (52), it is obtained that

$$u(t) = \sum_{K=0}^{\infty}\left[\frac{(t-t_i)^K}{K!}\right] U(k) = D^{-1}U(k) \tag{53}$$

5.1 Operational properties of differential transformation method

If $u(t)$ *and* $v(t)$ are two independent functions with time (t) where $U(k)$ and $V(k)$ are the transformed function corresponding to $u(t)$ and $v(t)$, then it can be proved from the fundamental mathematics operations performed by differential transformation that.

i. If $z(t) = u(t) \pm v(t)$, then $Z(k) = U(k) \pm V(k)$

ii. If $z(t) = \alpha u(t)$, then $Z(k) = \alpha U(k)$

iii. If $z(t) = \frac{du(t)}{dt}$, then $Z(k) = (k-1)\,U(k+1)$

iv. If $z(t)=u(t)v(t)$, then $Z(t)=\sum_{i=0}^{K}V(l)U(k-l)$

v. If $z(t)=u^{m}(t)$, then $Z(t)=\sum_{I=0}^{K}U^{m-1}(l)U(k-l)$

vi. If $z(t)=u^{n}(t)v^{n}(t)$, then $Z(t)=\sum_{l-0}^{k}\left[\sum_{j=0}^{l}\left[V(j)U(l-j)\right]\ \sum_{j=0}^{k-l}\left[V(j)U(k-l-j)\right]\right]$

vii. If $z(t)=u(t)v(t)$, then $Z(k)=\sum_{l=0}^{k}(l+1)V(l+1)U(k-l)$

5.2 Solution of the temporal nonlinear equation using differential transformation method

The above DTM described is applied to solve the temporal nonlinear differential equation. Applying DTM to Eq. (5), we have

$$\begin{aligned}&M\left[(p+2)(p+1)U(p+2)\right]+G\left[(p+1)U(p+1)\right]\\&+(K+C)U(p)-V\left[\sum_{m}^{p}\sum_{n=0}^{m}U(n)U(m-n)U(p-n)\right]=0\end{aligned}\tag{54}$$

Then

$$U(p+2)=\frac{1}{2(p+2)(p+1)M}\begin{Bmatrix}V\left[\sum_{m}^{p}\sum_{n=0}^{m}U(n)U(m-n)U(p-n)\right]\\-G\left[(p+1)U(p+1)\right]-(K+C)U(p)\end{Bmatrix}\tag{55}$$

For *p = 0, 1, 2, 3, 4, 5, 6, 7, 8*. We have the following

$$U(0)=A,\ U(1)=0,\ U(2)=\frac{A}{2M}\left\{VA^{2}-(K+C)\right\},\ U(3)=\frac{-GU(2)}{3M}$$

$$U(4)=\frac{1}{12M}\left[3VA^{2}U(2)-3GU(3)-(K+C)U(2)\right],\ U(5)=\frac{1}{20M}\left[3VA^{2}U(3)-4GU(4)-(K+C)U(3)\right]$$

$$U(6)=\frac{1}{30M}\left[3VA^{2}U(4)+3AU(2)-5GU(5)-(K+C)U(4)\right]$$

$$U(7)=\frac{1}{42M}\left[3VA^{2}U(5)+6VAU(2)U(3)-6GU(6)-(K+C)U(5)\right]\tag{56}$$

$$U(8)=\frac{1}{56M}\begin{bmatrix}3VA^{2}U(6)+6VAU(2)U(4)+3VAU^{3}(3)\\+VAU^{3}(2)-7GU(7)-(K+C)U(6)\end{bmatrix}$$

$$U(9)=\frac{1}{72M}\begin{bmatrix}3VA^2U(7)+6VAU(2)U(5)+6VAU(3)U(4)\\+3VAU^2(2)U(3)-8GU(8)-(K+C)U(7)\end{bmatrix}$$

$$U(10)=\frac{1}{90M}\begin{bmatrix}3VA^2U(8)+3VAU(2)U^2(3)+3VAU^2(4)+3VAU^2(2)U(4)\\+6VAU(2)U(6)-9GU(9)-(K+C)U(8)\end{bmatrix}$$

On applying the comparison function in Eqs. (20)-(36) made *G=0*for the clamped-clamped, clamped-simple and simple-simple supported structures, therefore the above equations reduced to

$$U(0)=A\;U(1)=0\;U(2)=\frac{A}{2M}\left\{VA^2-(K+C)\right\}\;U(3)=0$$

$$U(4)=\frac{1}{12M}\left[3VA^2U(2)-(K+C)U(2)\right]U(5)=0$$

$$U(6)=\frac{1}{30M}\left[3VA^2U(4)+3AU(2)-5GU(5)-(K+C)U(4)\right]U(7)=0$$

(57)

$$U(8)=\frac{1}{56M}\begin{bmatrix}3VA^2U(6)+6VAU(2)U(4)+3VAU^3(3)\\+VAU^3(2)-7GU(7)-(K+C)U(6)\end{bmatrix}U(9)=0$$

$$U(10)=\frac{1}{90M}\begin{bmatrix}3VA^2U(8)+3VAU(2)U^2(3)+3VAU^2(4)+3VAU^2(2)U(4)\\+6VAU(2)U(6)-9GU(9)-(K+C)U(8)\end{bmatrix}$$

Therefore,

$$\begin{aligned}u(t)=\sum_{k=0}^{\infty}U(k)t^k=&U(0)+U(1)t+U(2)t^2+U(3)t^3+U(4)t^4+U(5)t^5\\&+U(6)t^6+U(7)t^7+U(8)t^8+U(9)t^9+U(10)t^{10}+...\end{aligned}\tag{58}$$

$$
\begin{aligned}
u(t) = A &+ \frac{A}{2M}\left\{VA^2-(K+C)\right\}t^2 + \frac{A\left\{VA^2-(K+C)\right\}}{24M^2}\left[3VA^2-(K+C)\right]t^4 \\
&+ \frac{1}{30M}\left[\begin{array}{l}\frac{VA^3}{8M^2}\left[\left\{VA^2-(K+C)\right\}\left\{3VA^2-(K+C)\right\}\right]+\frac{3A^2}{2M}\left\{VA^2-(K+C)\right\} \\ -\frac{A(K+C)\left[\left\{VA^2-(K+C)\right\}\left\{3VA^2-(K+C)\right\}\right]}{24M^2}\end{array}\right]t^6 \\
&+ \frac{1}{56M}\left[\begin{array}{l}\frac{VA^2}{10M}\left[\begin{array}{l}\frac{VA^3}{8M^2}\left[\left\{VA^2-(K+C)\right\}\left\{3VA^2-(K+C)\right\}\right]+\frac{3A^2}{2M}\left\{VA^2-(K+C)\right\} \\ -\frac{A(K+C)\left[\left\{VA^2-(K+C)\right\}\left\{3VA^2-(K+C)\right\}\right]}{24M^2}\end{array}\right] \\ +\frac{3VA^2}{M}\left\{VA^2-(K+C)\right\}\frac{A\left\{VA^2-(K+C)\right\}}{24M^2}\left[3VA^2-(K+C)\right]+\frac{VA^4}{8M^3}\left\{VA^2-(K+C)\right\}^3 \\ -\frac{(K+C)}{30M}\left[\begin{array}{l}\frac{VA^3}{8M^2}\left[\left\{VA^2-(K+C)\right\}\left\{3VA^2-(K+C)\right\}\right]+\frac{3A^2}{2M}\left\{VA^2-(K+C)\right\} \\ -\frac{A(K+C)\left[\left\{VA^2-(K+C)\right\}\left\{3VA^2-(K+C)\right\}\right]}{24M^2}\end{array}\right]\end{array}\right]t^8 \\
&+ \frac{1}{90M}\left[\begin{array}{l}\frac{3VA^2}{56M}\left[\begin{array}{l}\frac{VA^2}{10M}\left[\begin{array}{l}\frac{VA^3}{8M^2}\left[\left\{VA^2-(K+C)\right\}\left\{3VA^2-(K+C)\right\}\right]+\frac{3A^2}{2M}\left\{VA^2-(K+C)\right\} \\ -\frac{A(K+C)\left[\left\{VA^2-(K+C)\right\}\left\{3VA^2-(K+C)\right\}\right]}{24M^2}\end{array}\right] \\ +\frac{3VA^2}{M}\left\{VA^2-(K+C)\right\}\frac{A\left\{VA^2-(K+C)\right\}}{24M^2}\left[3VA^2-(K+C)\right]+\frac{VA^4}{8M^3}\left\{VA^2-(K+C)\right\}^3 \\ -\frac{(K+C)}{30M}\left[\begin{array}{l}\frac{VA^3}{8M^2}\left[\left\{VA^2-(K+C)\right\}\left\{3VA^2-(K+C)\right\}\right]+\frac{3A^2}{2M}\left\{VA^2-(K+C)\right\} \\ -\frac{A(K+C)\left[\left\{VA^2-(K+C)\right\}\left\{3VA^2-(K+C)\right\}\right]}{24M^2}\end{array}\right]\end{array}\right] \\ +\left[\frac{VA^2\left\{VA^2-(K+C)\right\}}{8M^2}\left[3VA^2-(K+C)\right]\right]^2+\frac{3VA^3}{4M^2}\left\{VA^2-(K+C)\right\}^2\frac{A\left\{VA^2-(K+C)\right\}}{24M^2}\left[3VA^2-(K+C)\right] \\ +\frac{VA^2}{10M^2}\left\{VA^2-(K+C)\right\}\left[\begin{array}{l}\frac{VA^3}{8M^2}\left[\left\{VA^2-(K+C)\right\}\left\{3VA^2-(K+C)\right\}\right]+\frac{3A^2}{2M}\left\{VA^2-(K+C)\right\} \\ -\frac{A(K+C)\left[\left\{VA^2-(K+C)\right\}\left\{3VA^2-(K+C)\right\}\right]}{24M^2}\end{array}\right] \\ -\frac{(K+C)}{56M}\left[\begin{array}{l}\frac{VA^2}{10M}\left[\begin{array}{l}\frac{VA^3}{8M^2}\left[\left\{VA^2-(K+C)\right\}\left\{3VA^2-(K+C)\right\}\right]+\frac{3A^2}{2M}\left\{VA^2-(K+C)\right\} \\ -\frac{A(K+C)\left[\left\{VA^2-(K+C)\right\}\left\{3VA^2-(K+C)\right\}\right]}{24M^2}\end{array}\right] \\ +\frac{3VA^2}{M}\left\{VA^2-(K+C)\right\}\frac{A\left\{VA^2-(K+C)\right\}}{24M^2}\left[3VA^2-(K+C)\right]+\frac{VA^4}{8M^3}\left\{VA^2-(K+C)\right\}^3 \\ -\frac{(K+C)}{30M}\left[\begin{array}{l}\frac{VA^3}{8M^2}\left[\left\{VA^2-(K+C)\right\}\left\{3VA^2-(K+C)\right\}\right]+\frac{3A^2}{2M}\left\{VA^2-(K+C)\right\} \\ -\frac{A(K+C)\left[\left\{VA^2-(K+C)\right\}\left\{3VA^2-(K+C)\right\}\right]}{24M^2}\end{array}\right]\end{array}\right]\end{array}\right]t^{10}+\ldots
\end{aligned}
$$

(59)

Apart from the solution of the DTM given above is too long for practical applications, the method gives solution in the form of truncated series. This truncated series is periodic only in

a very small region. In order to make the solution periodic over a large range, we applied Cosine-after treatment (CAT-technique).
If the truncated series in Eq. (59) is expressed in even-power, only, of the independent variable *t*, i.e.

$$\Phi_N(t)=\sum_{k=0}^{N}U(2k)t^{2k}\quad U(2k+1)=0,\quad \forall k=0,1,...,\frac{N}{2}-1,\ \textit{where N is even} \tag{60}$$

The CAT- technique is based on the assumption that this truncated series can be expressed as another finite series in terms of the cosine-trigonometric functions with different amplitude and arguments

$$\Phi_N(t)=\sum_{j=1}^{N}\lambda_j cos\left(\Omega_j t\right),\quad \textit{where n is finite} \tag{61}$$

On expanding both sides of Eq. (61) as power series of *t* and equating the coefficient of like powers, we have

$$\begin{aligned}
&t^0;\quad \textstyle\sum_j^n \lambda_j = U(0),\\
&t^2;\quad \textstyle\sum_j^n \lambda_j\Omega_j^2 = -2!U(2),\\
&t^4;\quad \textstyle\sum_j^n \lambda_j\Omega_j^4 = 4!U(4),\\
&t^6;\quad \textstyle\sum_j^n \lambda_j\Omega_j^6 = -6!U(6),\\
&t^8;\quad \textstyle\sum_j^n \lambda_j\Omega_j^8 = 8!U(8),\\
&t^{10};\quad \textstyle\sum_j^n \lambda_j\Omega_j^{10} = -10!U(10),\\
&...
\end{aligned} \tag{61}$$

For practical application, it is sufficient to express the truncated series $\Phi_N(t)$ in terms of two cosines with different amplitudes and arguments as

$$\Phi_6(t)=\sum_{j=1}^{2}\lambda_j cos\left(\Omega_j t\right). \tag{62}$$

Therefore, we have

$$\lambda_1+\lambda_2=U(0) \tag{63a}$$

$$\lambda_1\Omega_1^2+\lambda_2\Omega_2^2=-2U(2) \tag{63b}$$

$$\lambda_1\Omega_1^4+\lambda_2\Omega_2^4=24U(4) \tag{63c}$$

$$\lambda_1\Omega_1^6+\lambda_2\Omega_2^6=-720U(6) \tag{63d}$$

On substituting the DTM results, we have

$$\lambda_1+\lambda_2=A \tag{64a}$$

$$\lambda_1\Omega_1^2+\lambda_2\Omega_2^2=-\frac{A}{M}\left\{VA^2-(K+C)\right\} \quad (64b)$$

$$\lambda_1\Omega_1^4+\lambda_2\Omega_2^4=\frac{A\left\{VA^2-(K+C)\right\}}{M^2}\left[3VA^2-(K+C)\right] \quad (64c)$$

$$\lambda_1\Omega_1^6+\lambda_2\Omega_2^6=-\frac{1}{24M}\left[\begin{array}{l}\dfrac{VA^3}{8M^2}\left[\left\{VA^2-(K+C)\right\}\left\{3VA^2-(K+C)\right\}\right]+\dfrac{3A^2}{2M}\left\{VA^2-(K+C)\right\}\\ -\dfrac{A(K+C)\left[\left\{VA^2-(K+C)\right\}\left\{3VA^2-(K+C)\right\}\right]}{24M^2}\end{array}\right] \quad (64d)$$

On solving the above Eq. (64a-64d), we have

$$\lambda_1=A\left\{\frac{4(K+C)-5VA^2+\sqrt{\left[2(K+C)-3VA^2\right]\left[8(K+C)-9VA^2\right]}}{2\sqrt{\left[2(K+C)-3VA^2\right]\left[8(K+C)-9VA^2\right]}}\right\} \quad (65a)$$

$$\lambda_2=-A\left\{\frac{4(K+C)-5VA^2-\sqrt{\left[2(K+C)-3VA^2\right]\left[8(K+C)-9VA^2\right]}}{2\sqrt{\left[2(K+C)-3VA^2\right]\left[8(K+C)-9VA^2\right]}}\right\} \quad (65b)$$

$$\Omega_1=\pm\sqrt{\frac{5(K+C)-6VA^2-\sqrt{\left[2(K+C)-3VA^2\right]\left[8(K+C)-9VA^2\right]}}{M}} \quad (65c)$$

$$\Omega_2=\pm\sqrt{\frac{5(K+C)-6VA^2+\sqrt{\left[2(K+C)-3VA^2\right]\left[8(K+C)-9VA^2\right]}}{M}} \quad (65d)$$

Therefore, the approximated periodic solution for *u(t)* is given as

$$u(t)=A\left\{\frac{4(K+C)-5VA^2+\sqrt{\left[2(K+C)-3VA^2\right]\left[8(K+C)-9VA^2\right]}}{2\sqrt{\left[2(K+C)-3VA^2\right]\left[8(K+C)-9VA^2\right]}}\right\}\cos\left\{\sqrt{\frac{5(K+C)-6VA^2-\sqrt{\left[2(K+C)-3VA^2\right]\left[8(K+C)-9VA^2\right]}}{M}}\right\}t$$
$$-A\left\{\frac{4(K+C)-5VA^2-\sqrt{\left[2(K+C)-3VA^2\right]\left[8(K+C)-9VA^2\right]}}{2\sqrt{\left[2(K+C)-3VA^2\right]\left[8(K+C)-9VA^2\right]}}\right\}\cos\left\{\sqrt{\frac{5(K+C)-6VA^2+\sqrt{\left[2(K+C)-3VA^2\right]\left[8(K+C)-9VA^2\right]}}{M}}\right\}t \quad (66)$$

(i) Clamped-clamped (doubly clamped)

$$w(x,t)=A\left\{\begin{array}{l}\left\{\begin{array}{l}\left\{\dfrac{4(K+C)-5VA^2+\sqrt{\left[2(K+C)-3VA^2\right]\left[8(K+C)-9VA^2\right]}}{2\sqrt{\left[2(K+C)-3VA^2\right]\left[8(K+C)-9VA^2\right]}}\right\}\\ \times cos\left\{\sqrt{\dfrac{5(K+C)-6VA^2-\sqrt{\left[2(K+C)-3VA^2\right]\left[8(K+C)-9VA^2\right]}}{M}}\right\}t\end{array}\right\}\\ -\left\{\begin{array}{l}\left\{\dfrac{4(K+C)-5VA^2-\sqrt{\left[2(K+C)-3VA^2\right]\left[8(K+C)-9VA^2\right]}}{2\sqrt{\left[2(K+C)-3VA^2\right]\left[8(K+C)-9VA^2\right]}}\right\}\\ \times cos\left\{\sqrt{\dfrac{5(K+C)-6VA^2+\sqrt{\left[2(K+C)-3VA^2\right]\left[8(K+C)-9VA^2\right]}}{M}}\right\}t\end{array}\right\}\end{array}\right\}\left\{\left(\frac{x}{L}\right)^2\left(1-\frac{x}{L}\right)^2\right\} \tag{67}$$

(ii) Pinned-Pinned structure

$$w(x,t)=A\left\{\begin{array}{l}\left\{\begin{array}{l}\left\{\dfrac{4(K+C)-5VA^2+\sqrt{\left[2(K+C)-3VA^2\right]\left[8(K+C)-9VA^2\right]}}{2\sqrt{\left[2(K+C)-3VA^2\right]\left[8(K+C)-9VA^2\right]}}\right\}\\ \times cos\left\{\sqrt{\dfrac{5(K+C)-6VA^2-\sqrt{\left[2(K+C)-3VA^2\right]\left[8(K+C)-9VA^2\right]}}{M}}\right\}t\end{array}\right\}\\ -\left\{\begin{array}{l}\left\{\dfrac{4(K+C)-5VA^2-\sqrt{\left[2(K+C)-3VA^2\right]\left[8(K+C)-9VA^2\right]}}{2\sqrt{\left[2(K+C)-3VA^2\right]\left[8(K+C)-9VA^2\right]}}\right\}\\ \times cos\left\{\sqrt{\dfrac{5(K+C)-6VA^2+\sqrt{\left[2(K+C)-3VA^2\right]\left[8(K+C)-9VA^2\right]}}{M}}\right\}t\end{array}\right\}\end{array}\right\}\left\{sin\frac{n\pi x}{L}\right\} \tag{68}$$

Note: *M, K, C and V are respective integral values of the respective space functions of the respective boundary conditions and structure considered.*

6 Results and Discussion

Figures (2-5) show the first five normalized mode shapes of the beams for clamped-clamped, simple-simple, clamped-simple and clamped-free supports. Also, the figures show the deflections of the beams along the beams' span at five different buckled and mode shapes.

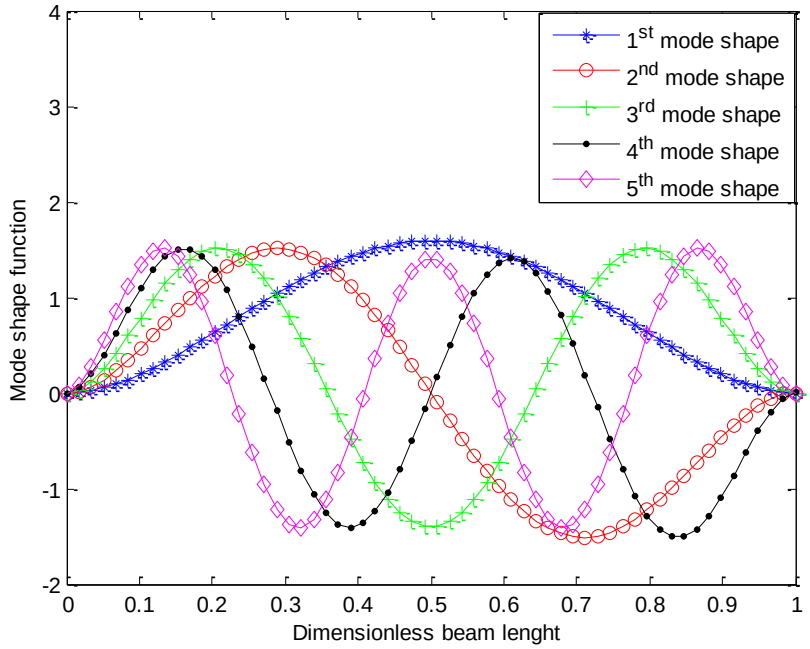

Figure 2 The first five normalized mode shaped of the beams under clamped-clamped supports

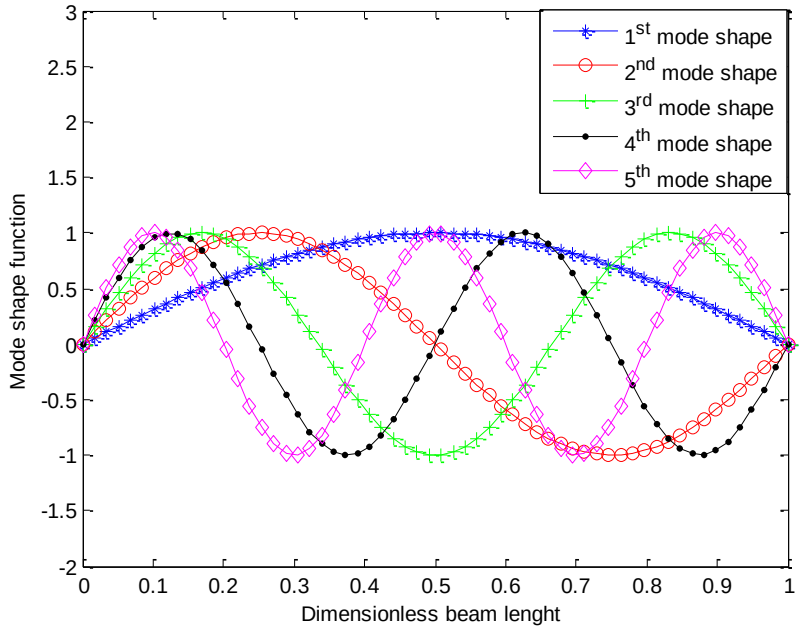

Figure 3 The first five normalized mode shaped of the beams under simple-simple supports

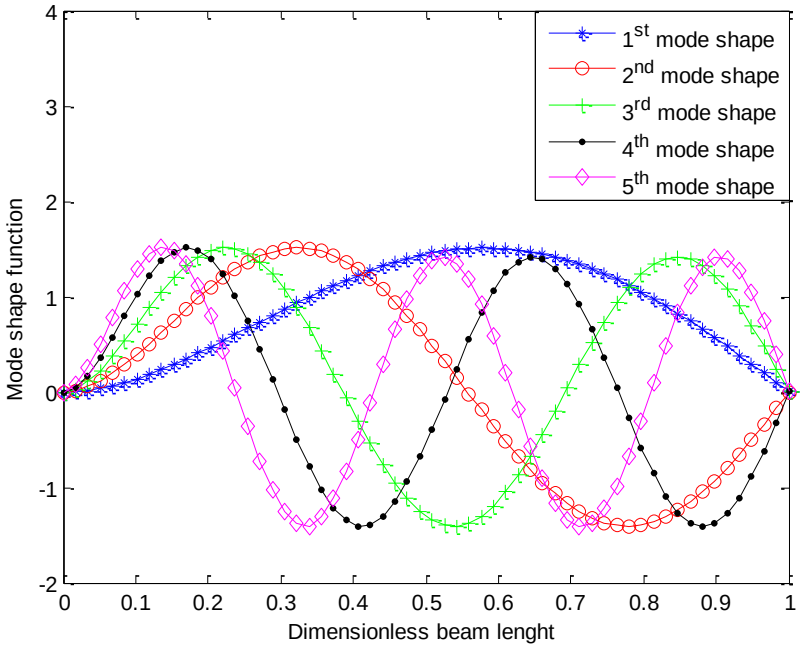

Figure 4 The first five normalized mode shapes of the beams under clamped-simple supports

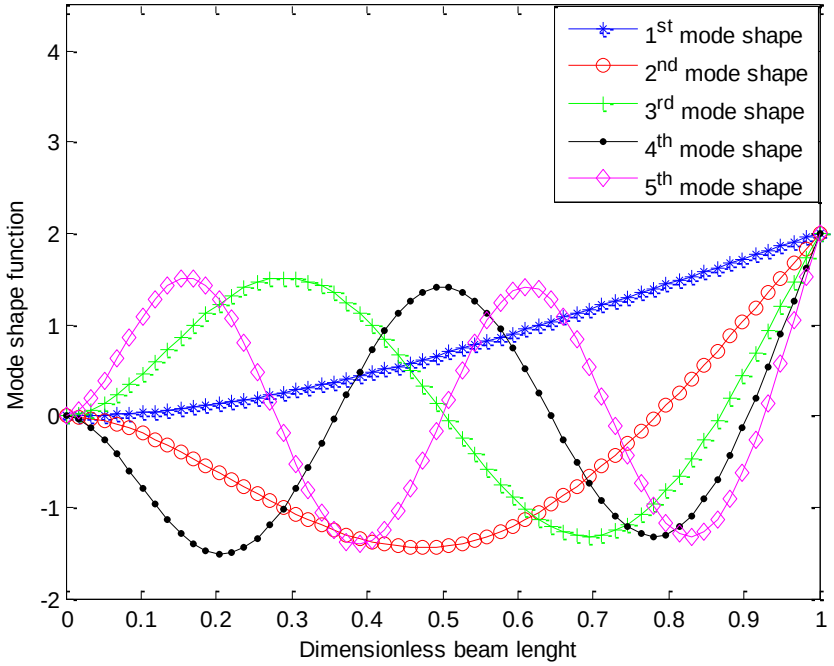

Figure 5 First five normalized mode shaped of the beams under clamped-free (cantilever) supports

Figures. (6-9) show the comparison of hyperbolic-trigonometric and the polynomial functions for the normalized mode shapes of the beams for clamped-clamped, simple-simple, clamped-simple and clamped-free supports. The figures depict the validity of the developed polynomial functions in this work as there are very good agreements between the hyperbolic-trigonometric and the developed polynomial functions.

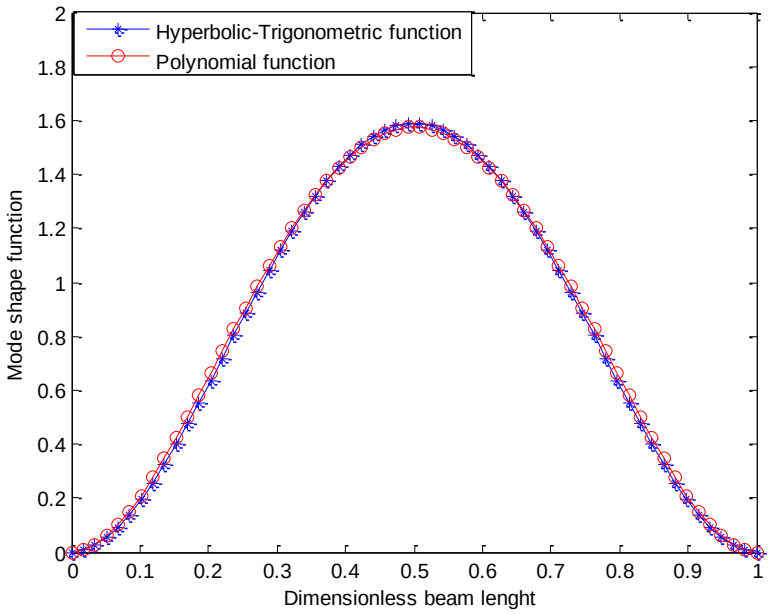

Figure 6 Normalized mode shaped of the structures under clamped-clamped supports for Hyperbolic-Trigonometric and Polynomial functions

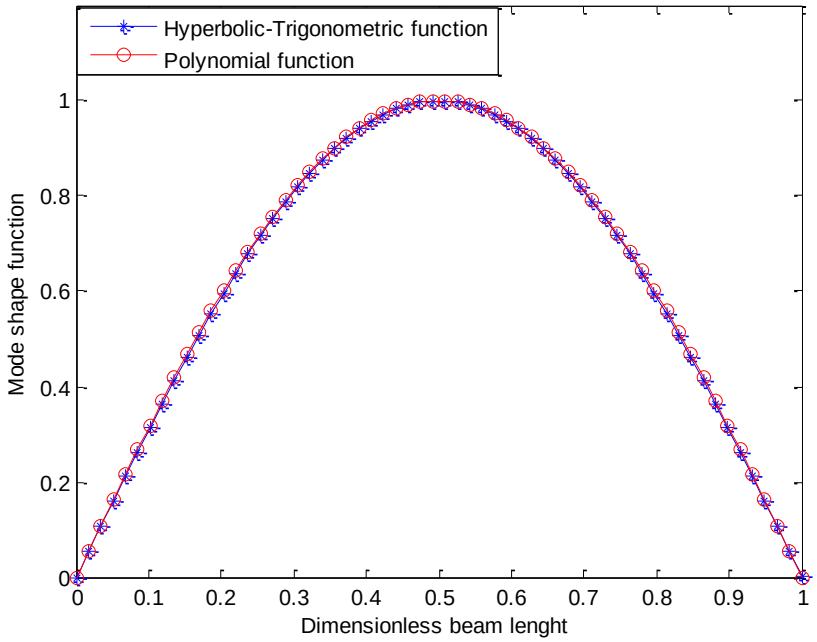

Figure 7 Normalized mode shaped of the structures under simple-simple supports for Hyperbolic-Trigonometric and Polynomial functions

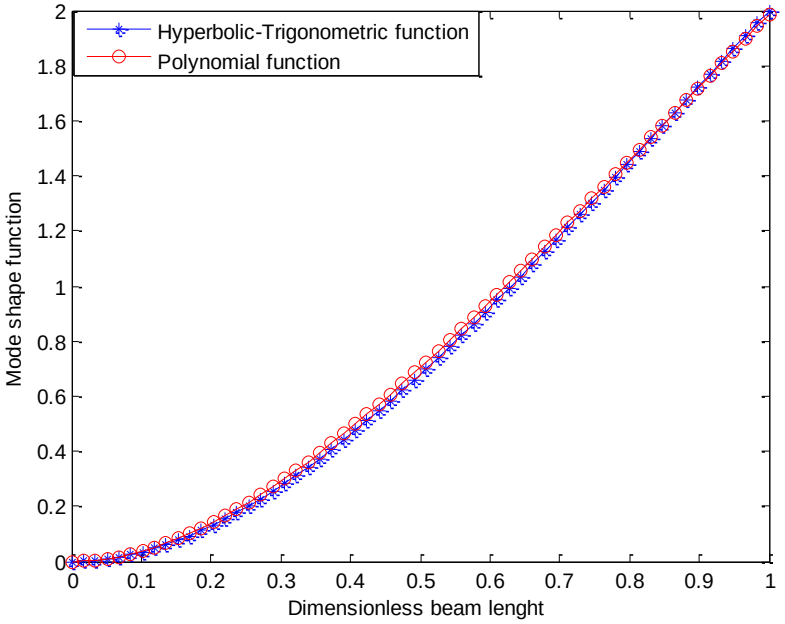

Figure 8 Normalized mode shaped of the structures under clamped-free supports for Hyperbolic-Trigonometric and Polynomial functions

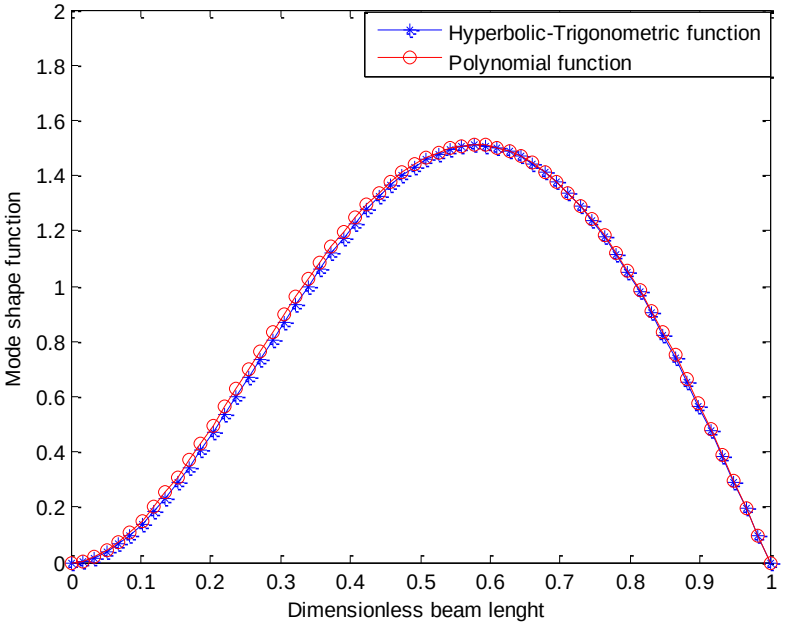

Figure 9 Normalized mode shaped of the structures under clamped-simple supports for Hyperbolic-Trigonometric and Polynomial functions

Figure (10) illustrates the effects of boundary conditions on the nonlinear amplitude-frequency response curves of the pipe. Also, the figure shows the variation of frequency ratio of the pipe with the dimensionless maximum amplitude of the structure under different boundary conditions. From, the result, it shown that frequency ratio is highest in the beam which is clamped-free (cantilever) supported beam and lowest with clamped-clamped beam.

The lowest frequency ratio of the clamped-clamped beam is due to high stiffness of the beam with this type of boundary conditions in comparison with other types of boundary conditions. The fundamental linear vibration frequency is the lowest root of the resulting characteristics equation. It can be seen from the figure, in contrast to linear systems, the nonlinear frequency is a function of amplitude so that the larger the amplitude, the more pronounced the discrepancy between the linear and the nonlinear frequencies becomes.

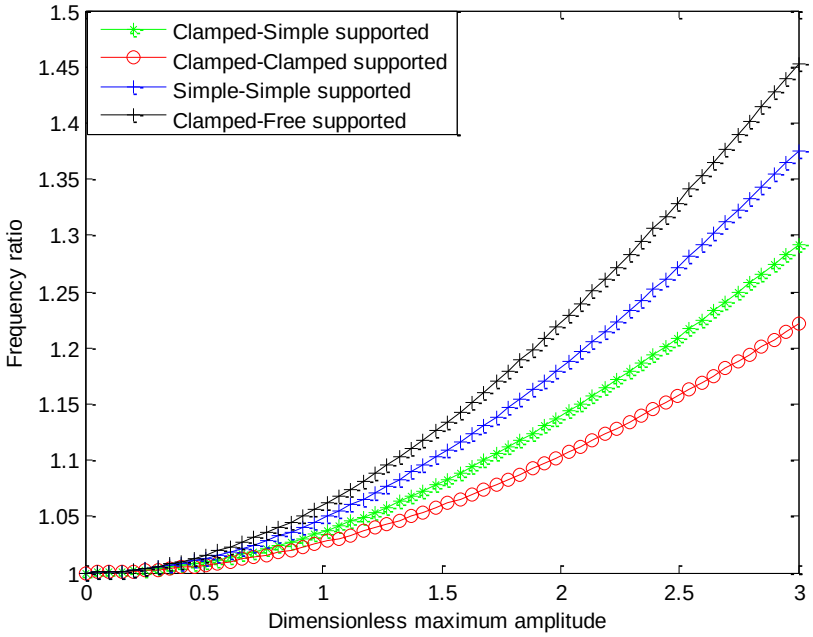

Figure 10 Effects of boundary conditions on the nonlinear amplitude-frequency response curves of the pipe

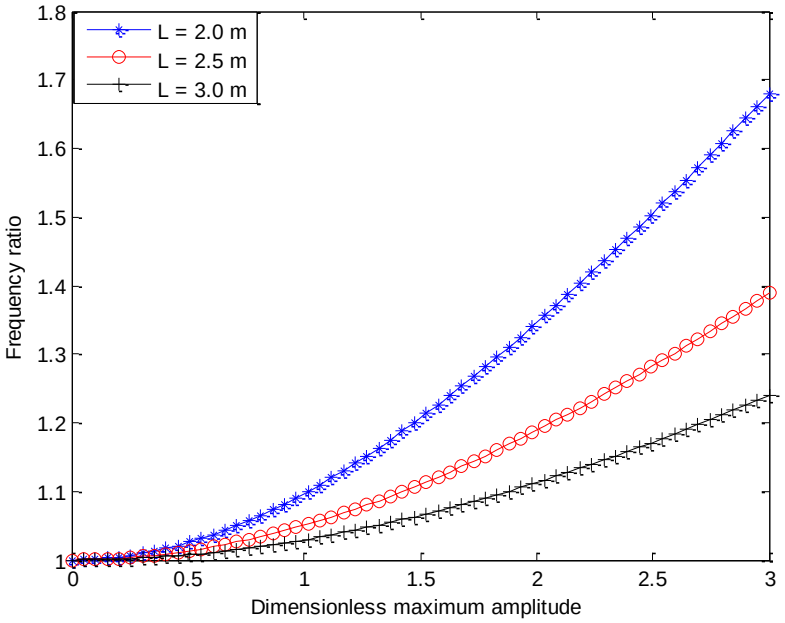

Figur 11 Effects of boundary pipe length on the nonlinear amplitude-frequency response curves of the pipe

Figure (11) show the effects of pipe length on the nonlinear amplitude-frequency response curves of the pipe. It is observed that with increase of the length or by extension, the aspect ratio of the pipe, the nonlinear vibration frequencies of the structure decreases while nonlinear vibration frequencies increases with the increase in the fluid-flow velocity.

Figure (12) shows effects of fluid-flow velocity on the nonlinear amplitude-frequency response curves of pipe. It is observed that with increase of the length or by extension, the aspect ratio of the pipe, the nonlinear vibration frequencies of the structure decreases while nonlinear vibration frequencies increases with the increase in the fluid-flow velocity.

Figure (13) show the comparison of the results of exact analytical solution and the results of the present study for the linear models while Figure (14) presents the comparison of numerical results models and the results of present work for the nonlinear models. From the results, it could been seen that good agreements are established reached and good agreements are established reached.

Figure (15) illustrates the midpoint deflection time history for the nonlinear analysis of SWCBT when *Kn=0.03* and *U= 100 m/s* while Figure (16) presents the midpoint deflection time history for the nonlinear analysis of SWCBT when *Kn=0.03* and *U= 500 m/s*.

Also, Figure (17) depicts the midpoint deflection time history for the linear analysis of CBT when *Kn=0.03*and *U= 500 m/s* The Knudsen number measures the slip effects of the fluid on the flow and consequently on the vibration induced by the flow. It should be pointed out that the Knudsen number predicts various flow regimes in the fluid-conveying nanotube.

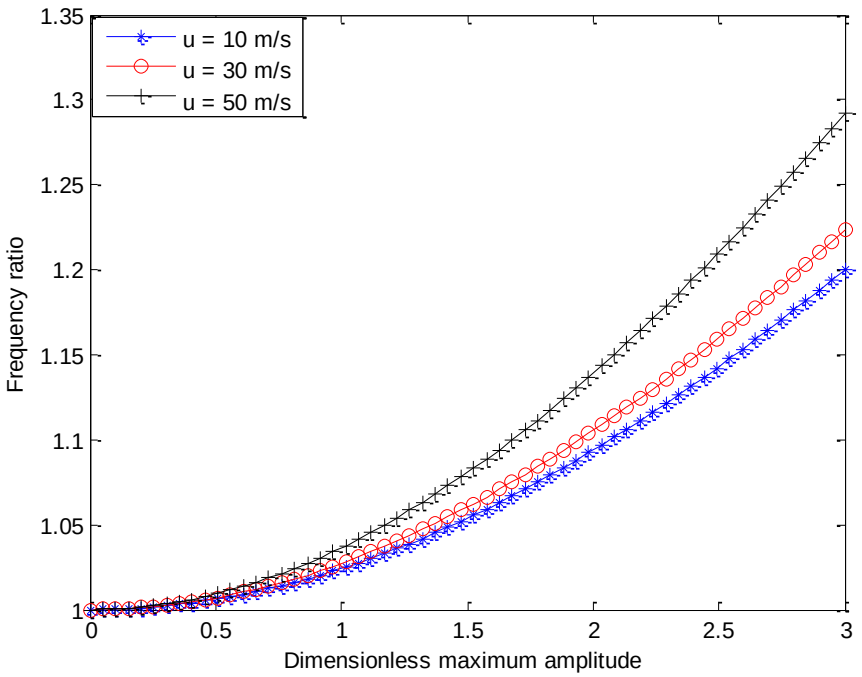

Figure 12 Effects of fluid-flow velocity on the nonlinear amplitude-frequency response curves of pipe

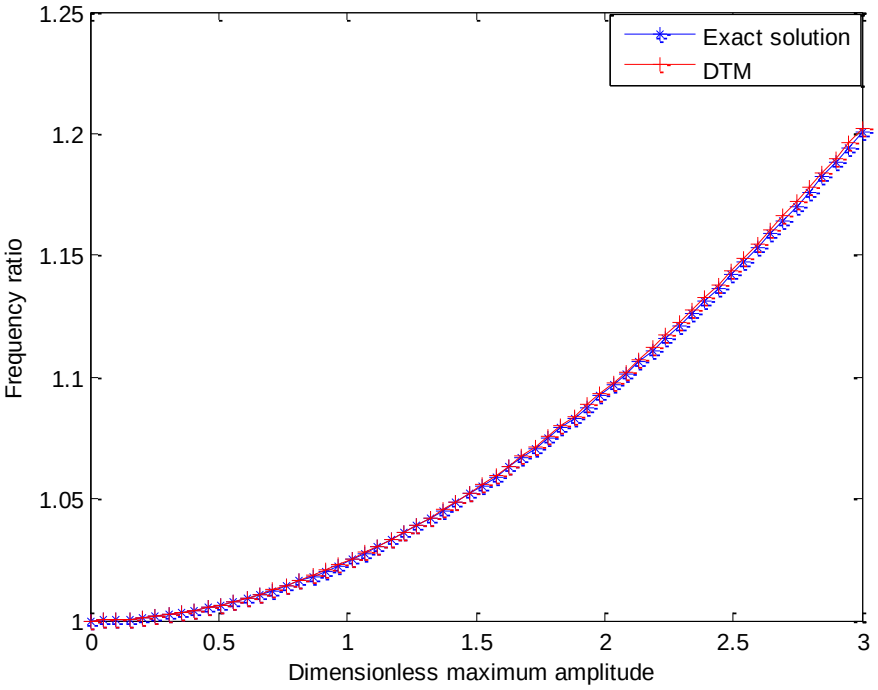

Figure 13 Comparison between the obtained results and the exact solution for the linear vibration

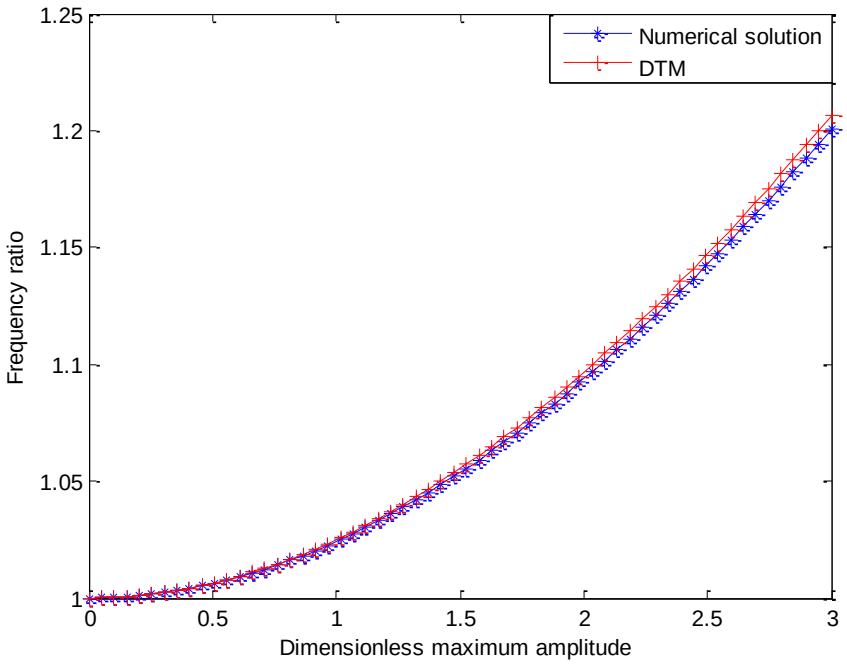

Figure 14 Comparison between the obtained results and the numerical solution for the nonlinear vibration

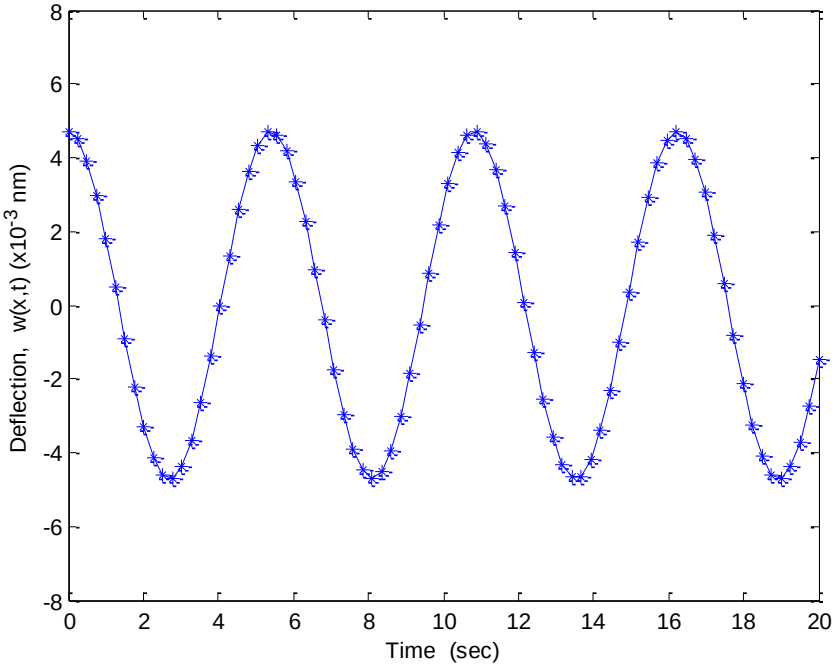

Figure15 Midpoint deflection time history for the nonlinear analysis of SWCBT When Kn=0.03 and U= 100 m/s

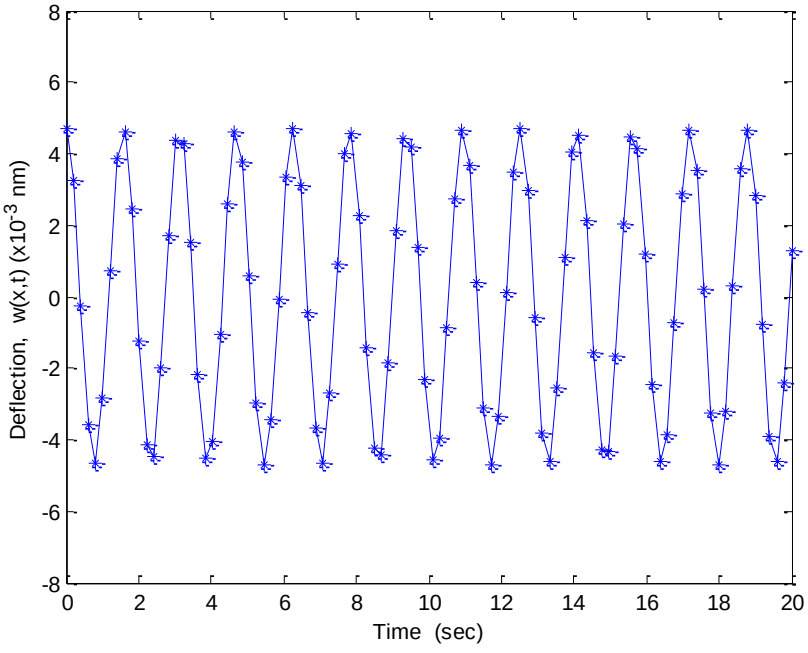

Figure 16 Midpoint deflection time history for the nonlinear analysis of SWCBT when Kn=0.03 and U= 500 m/s

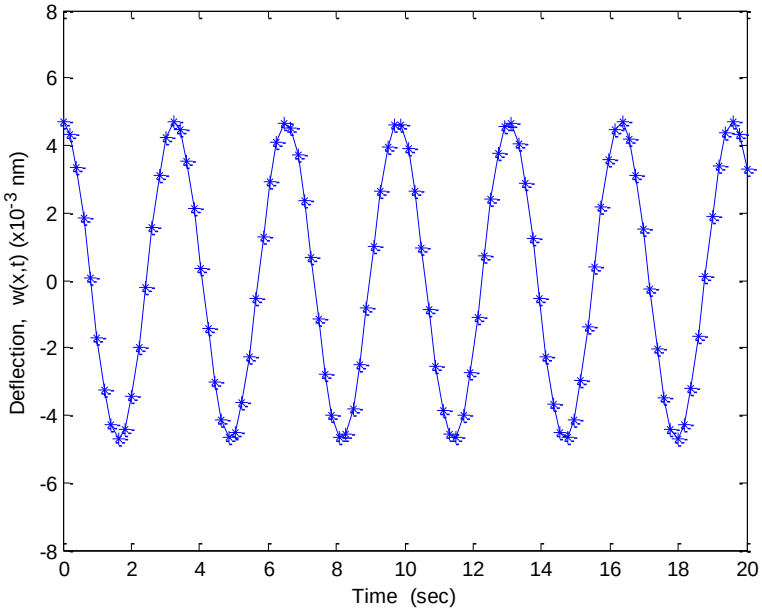

Figure 17 Midpoint deflection time history for the linear analysis of SWCBT when Kn=0.03 and U= 500 m/s

Figure (18) shows the comparison of the linear vibration with nonlinear vibration of the SWCNT. It could be seen in the figure that the discrepancy between the linear and nonlinear amplitudes increases with increment of the maximum vibration.

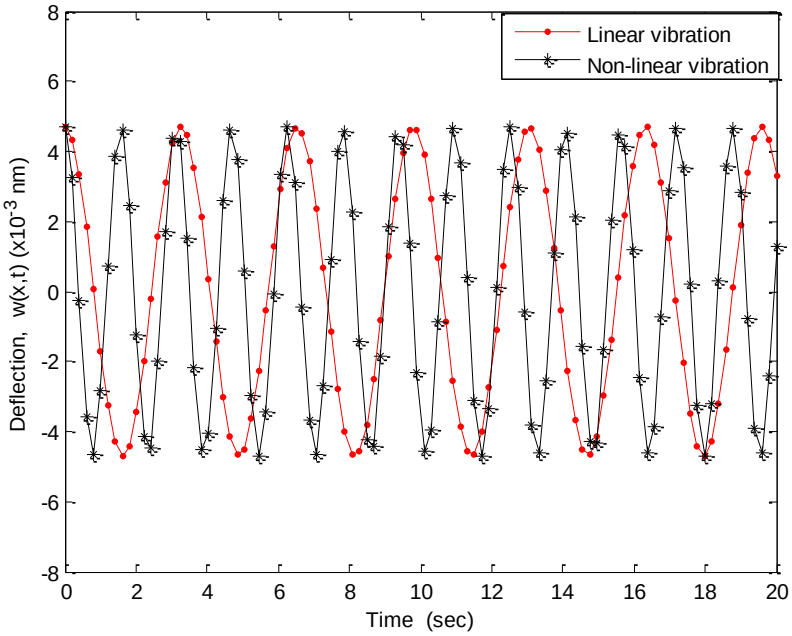

Figure 18 Comparison of midpoint deflection time history for the linear and nonlinear analysis of CBT when Kn=0.03 and U= 500 m/s

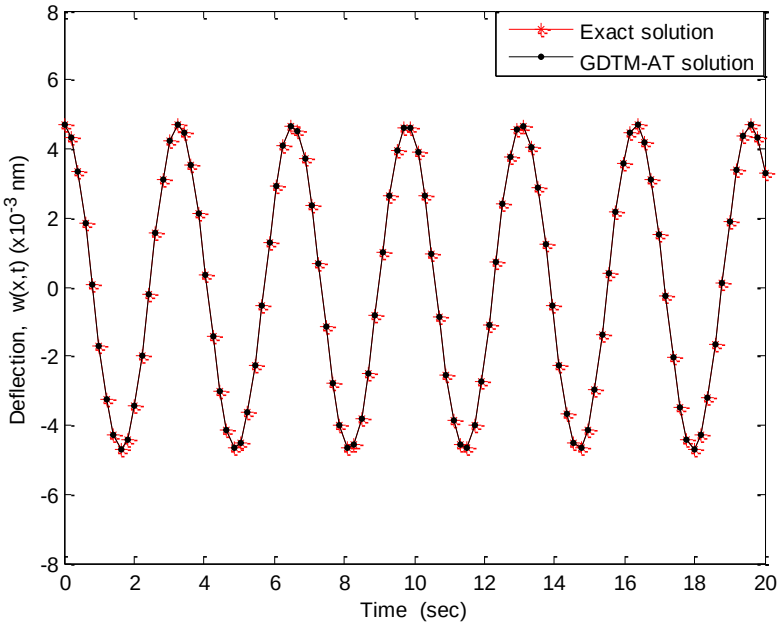

Figure 19 Comparison between the obtained results and the exact solution for the linear vibration

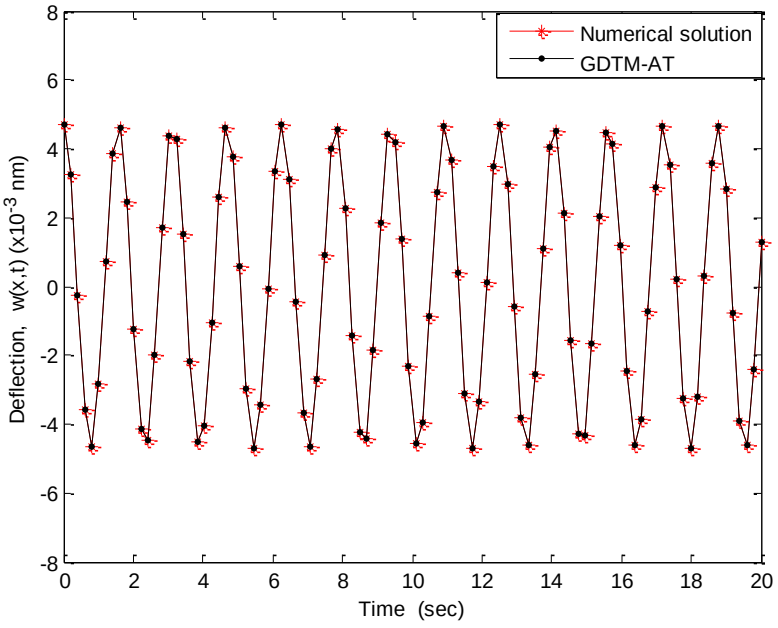

Figure 20 Comparison between the obtained results and the numerical solution for the nonlinear vibration

Figure (19) and (20) show the comparison of the results of exact analytical solution and the results of the present study for the linear models while Figure (14) presents the comparison of numerical results models and the results of present work for the nonlinear models.
The results show that good agreements are established reached and good agreements are established reached.

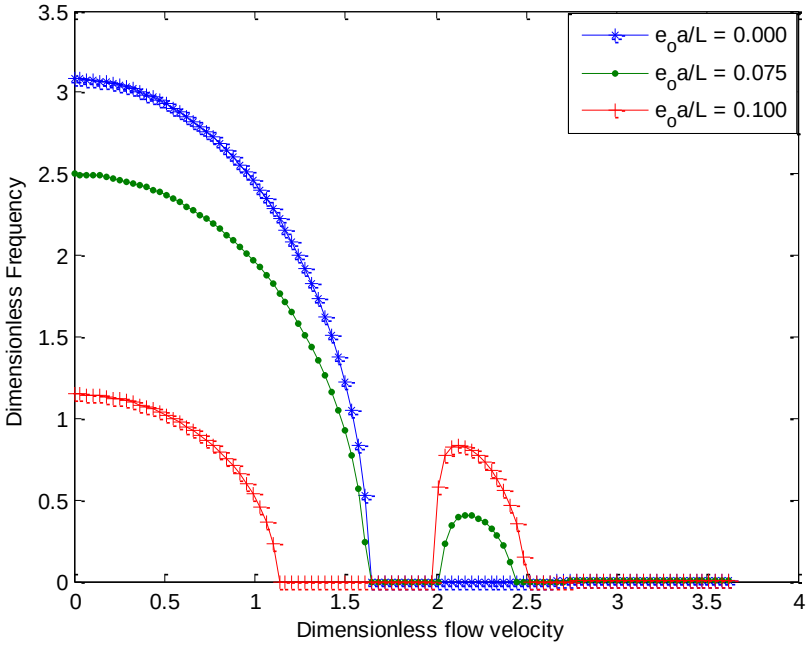

Figure 21 Effects of nonlocal parameter on the natural frequency of the nonlinear vibration

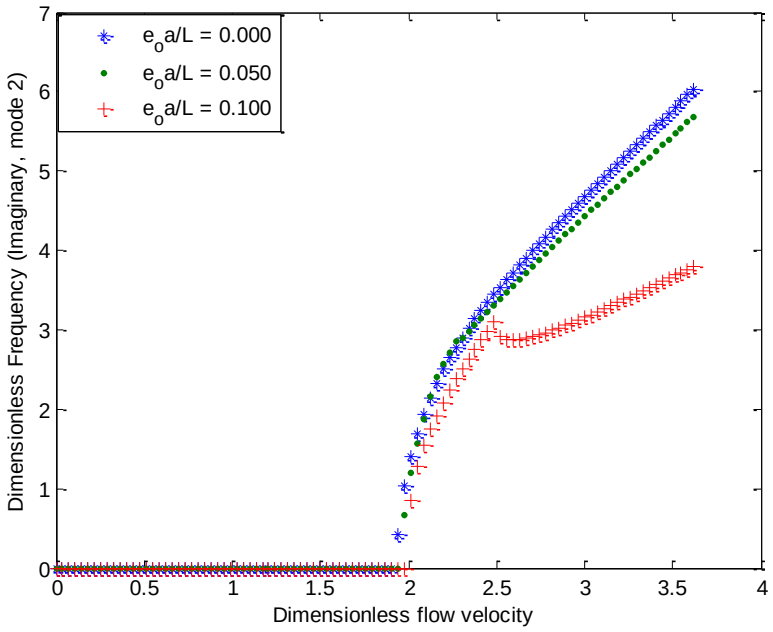

Figure 22 Effects of nonlocal parameter on the natural frequency of the nonlinear vibration

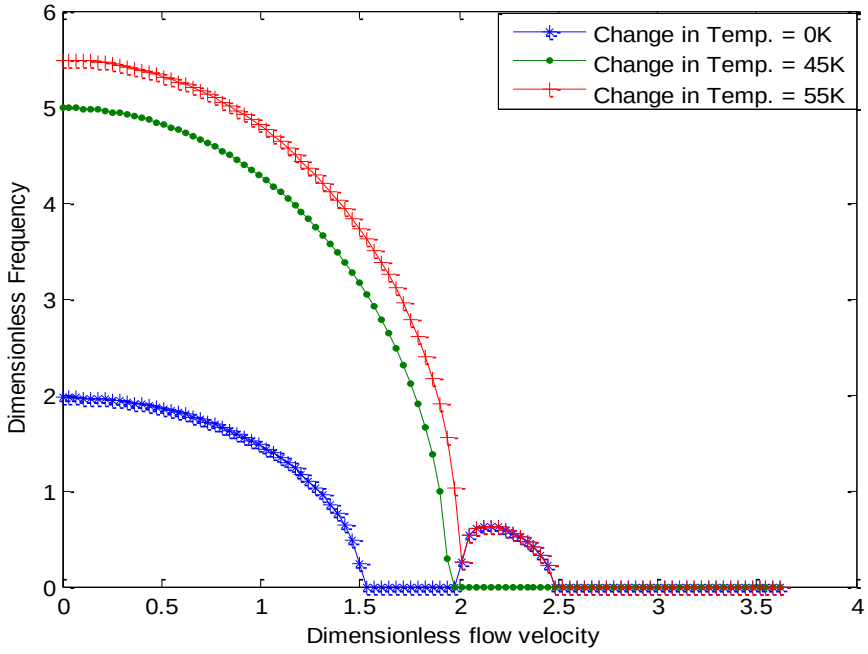

Figure 23 Effects of temperature change on the natural frequency of the structure vibration

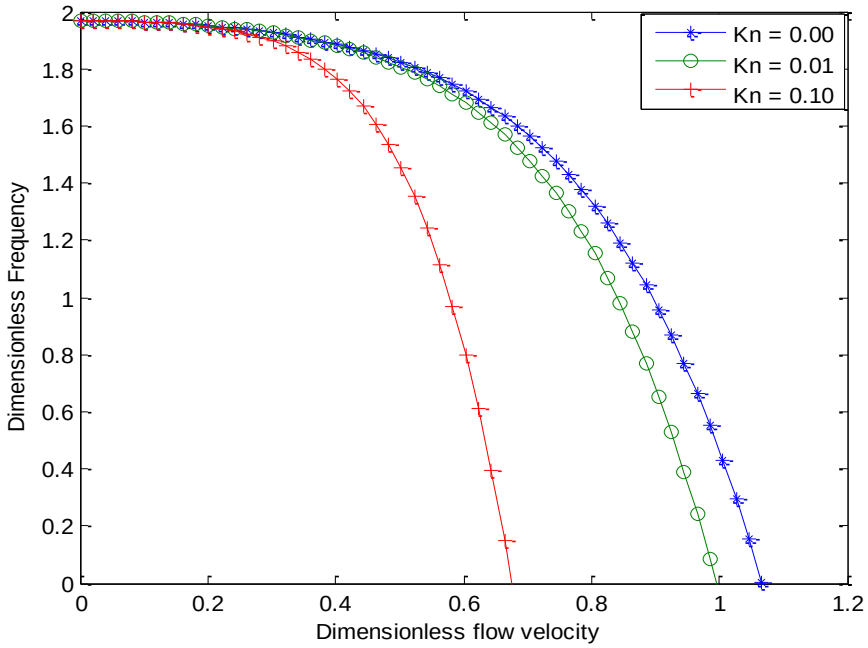

Figure 24 Effects of Knudsen number on the dimensionless frequency of simply supported single-walled nanotube

The studies and the investigations of the dynamic and stability behaviours of the structure are largely dependent on the effects of fluid flow velocity, amplitude on the natural frequencies of the vibration. Effects of nonlocal parameter and temperature on the vibration of the nanotube are shown in Figures (10-12). It is depicted that increase in the slip parameter leads to decrease in the frequency of vibration of the structure and the critical velocity of the conveyed fluid.

It should be pointed out as shown in the figures that the zero value for the nonlocal parameter, i.e. $e_o a = 0$, represents the results of the classical Euler-Bernoulli model which has the highest frequency and critical fluid velocity (a point where the structure starts to experience instability). When the flow velocity of the fluid attains the critical velocity, both the real and imaginary parts of the frequency are equal to zero. Also, the figures present the critical speeds corresponding to the divergence conditions for different values of the nonlocal parameters. It is shown in Figures (10) and (11), the real and imaginary parts of the eigenvalues related to the two lowest modes with different nanotube parameters.
Figure (12) shows the effects of temperature change on the frequencies of the CNT. From the figure, as the temperature change increases, the natural frequencies and the critical flow velocity of the structure increase. Effects of slip parameter, Knudsen number on the dimensionless frequency ratio of the nanotube are shown in Figure (13).
It is depicted that increase in the slip parameter leads to decrease in the dimensionless frequency ratio of vibration of the SWCNT. It should be pointed out that the Knudsen number predicts various flow regimes in the fluid-conveying nanotube. The Knudsen number with zero value has the highest frequency as shown in the figure. As the Knudsen number increases, the bending stiffness of the nanotube decreases and in consequent, the critical continuum flow velocity decreases as the curves shift to the lowest frequency zone.

7 Conclusion

In this work, analytical solutions to the nonlinear equations arising in flow-induced vibration of in pipes, micro-pipes and nanotubes using Galerkin-differential transformation method with aftertreatment technique have been developed. From the analysis, it was established that increase of the length and aspect ratio of the fluid-conveying structures result in decrease the nonlinear vibration frequencies of the structure while increase in the fluid-flow velocity causes increase in nonlinear vibration frequencies of the structures. Also, increase in the slip parameter leads to decrease in the frequency of vibration of the structure and the critical velocity of the conveyed fluid while increase in the slip parameter leads to decrease in the dimensionless frequency ratio of vibration of the structure.
As the Knudsen number increases, the bending stiffness of the nanotube decreases and in consequent, the critical continuum flow velocity decreases as the curves shift to the lowest frequency zone. The results show that the alteration of nonlinear flow-induced frequency from linear frequency is significant as the amplitude, flow velocity, and aspect ratio increase. The developed analytical solutions are compared with the numerical results for the non-linear models and the results of exact analytical solution for the linear models and good agreements are established. The analytical solutions can serve as a starting point for a better understanding of the relationship between the physical quantities of the problems as it provides continuous physical insights into the problems than pure numerical or computation methods.

References

[1] Benjamin, T. B., “Dynamics of a System of Articulated Pipes Conveying Fluid”, I. Theory. Proc. R. Soc. A Vol. 261, pp. 487–499, (1961).

[2] Housner, G. W., Dodds, H. L., and Runyan, H., “Effect of High Velocity Fluid Flow in the Bending Vibration and Static Divergence of Simply Supported Pipes”, National Aeronautics and Space Administration Report NASA TN D- 2870, June (1965).

[3] Holmes, P. J., "Pipe Supported at Both Ends Cannot Flutter", Journal of Applied Mechanics, Vol. 45, pp. 669-672, (1978).

[4] Semler., C., Li, G. X., and Paidoussis, M. P., "The Non-linear Equations of Motion of Pipes Conveying Fluid", Journal of Sound and Vibration, Vol. 169, pp. 577-599, (1994).

[5] Paidoussis, M. P., "Dynamics of Flexible Slender Cylinders in Axial Flow", Journal of Fluid Mechanics, Vol. 26, pp. 717-736, (1966).

[6] Paidoussis, M. P., and Deksnis, E. B., "Articulated Models of Cantilevers Conveying Fluid, the Study of Paradox", Journal of Mechanical Engineering Science, Vol. 12, pp. 288-300, (1970).

[7] Rinaldi, S., Prabhakar, S., Vengallatore, S., and Paıdoussis, M. P., "Dynamics of Microscale Pipes Containing Internal Fluid Flow: Damping, Frequency Shift, and Stability", J. Sound Vib. Vol. 329, pp. 1081–1088, (2010).

[8] Akgoz, B., and Civalek, O., "Free Vibration Analysis of Axially Functionally Graded Tapered Bernoulli–Euler Microbeams Based on the Modified Couple Stress Theory", Compos. Struct. Vol. 98, pp. 314–322, (2013).

[9] Xia, W., and Wang, L., "Microfluid-induced Vibration and Stability of Structures Modeled as Microscale Pipes Conveying Fluid Based on Non-classical Timoshenko Beam Theory", Microfluid Nanofluid, Vol. 9, pp. 955–962, (2010).

[10] Ahangar, S., Rezazadeh, G., Shabani, R., Ahmadi, G., and Toloei, A., "On the Stability of a Microbeam Conveying Fluid Considering Modified Couple Stress Theory", Int. Journal Mech. Vol. 7, pp. 327–342, (2011).

[11] Yin, L., Qian, Q., and Wang, L., "Strain Gradient Beam Model for Dynamics of Microscalepipes Conveying Fluid", Appl. Math. Model. Vol. 35, pp. 2864–2873, (2011).

[12] Sahmani, S., Bahrami, M., and Ansari, R., "Nonlinear Free Vibration Analysis of Functionally Graded Third-order Shear Deformable Microbeams Based on the Modified Strain Gradient Elasticity Theory", Compos. Struct. Vol. 110, pp. 219–230, (2014).

[13] Akgoz, B., and Civalek, O., "Buckling Analysis of Functionally Graded Microbeams Based on the Strain Gradient Theory", Acta Mech. Vol. 224, pp. 2185–2201, (2013).

[14] Zhao, J., Zhou, S., Wang, B., and Wang, X., "Nonlinear Microbeam Model Based on Strain Gradient Theory", Appl. Math. Model. Vol. 36, pp. 2674–2686, (2012).

[15] Kong, S. L., Zhou, S. J., Nie, Z. F., and Wang, K., "Static and Dynamic Analysis of Micro-beams Based on Strain Gradient Elasticity Theory", Int. J. Eng. Sci. Vol. 47, pp. 487–498, (2009).

[16] Setoodeh, R., and Afrahhim, S., "Nonlinear Dynamic Analysis of FG Micro-pipes Conveying Fluid Based on Strain Gradient Theory", Composite Structures, Vol. 116, pp. 128-135, (2014).

[17] Yoon, G., Ru, C.Q., and Mioduchowski, A., "Vibration and Instability of Carbon Nanotubes Conveying Fluid", Journal of Applied Mechanics, Transactions of the ASME, Vol. 65, No. 9, pp. 1326–1336, (2005).

[18] Yan, Y., Wang, W.Q., and Zhang, L.X., "Nonlocal Effect on Axially Compressed Buckling of Triple-walled Carbon Nanotubes under Temperature Field", Journal of Applied Math and Modelling, Vol. 34, pp. 3422–3429, (2010).

[19] Murmu, T., and Pradhan, S.C., "Thermo-mechanical Vibration of Single-walled Carbon Nanotube Embedded in an Elastic Medium Based on Nonlocal Elasticity Theory", Computational Material Science, Vol. 46, pp. 854–859, (2009).

[20] Yang, H.K., and Wang, X., "Bending Stability of Multi-wall Carbon Nanotubes Embedded in an Elastic Medium", Modeling and Simulation in Materials Sciences and Engineering, Vol. 14, pp. 99–116, (2006).

[21] Yoon, J., Ru, C.Q., and Mioduchowski, A., "Vibration of an Embedded Multiwall Carbon Nanotube", Composites Science and Technology, Vol. 63, No. 11, pp. 1533–1542, (2003).

[22] Chang, W.J., and Lee, H.L., "Free Vibration of a Single-walled Carbon Nanotube Containing a Fluid Flow using the Timoshenko Beam Model", Physics Letter A, Vol. 373, No. 10, pp. 982–985, (2009).

[23] Zhang, Y., Liu, G., and Han, X., "Transverse Vibration of Double-walled Carbon Nanotubes under Compressive Axial Load", Applied Physics Letter A, Vol. 340, No. 1-4, pp. 258–266, (2005).

[24]GhorbanpourArani, A., Zarei, M.S., Mohammadimehr, M., Arefmanesh, A., and Mozdianfard, M.R., "The Thermal Effect on Buckling Analysis of a DWCNT Embedded on the Pasternak Foundation", Physica E, Vol. 43, pp. 1642–1648, (2011).

[25] Sobamowo, M.G., "Thermal Analysis of Longitudinal Fin with Temperature-dependent Properties and Internal Heat Generation using Galerkin's Method of Weighted Residual", Applied Thermal Engineering, Vol. 99, pp. 1316–1330, (2016).

[26] Zhou, J.K., "Differential Transformation and its Applications for Electrical Circuits", Huazhong University Press, Wuhan, China, (1986).

[27] Venkatarangan, S.N., and Rajakshmi, K., "A Modification of Adomian's Solution for Nonlinear Oscillatory Systems", Comput. Math. Appl. Vol. 29, pp. 67-73, (1995).

[28] Jiao, Y.C., Yamamoto, Y., Dang, C., and Hao, Y., "An Aftertreatment Technique for Improving the Accuracy of Adomian's Decomposition Method", Comput. Math. Appl. Vol. 43, pp. 783-798, (2002).

[29] Elhalim, A., and Emad, E., "A New Aftertratment Technique for Differential Transformation Method and its Application to Non-linear Oscillatory System", International Journal of Non-linear Science, Vol. 8, No. 4, pp. 488-497, (2009).

[30] Eringen, A.C., "On Differential Equations of Nonlocal Elasticity and Solutions of Screw Dislocation and Surface Waves", Journal of Applied Physics, Vol. 54, No. 9, pp. 4703–4710, (1983).

[31] Eringen, A.C., "Linear Theory of Nonlocal Elasticity and Dispersion of Plane Waves", International Journal of Engineering Science, Vol. 10, No. 5, pp. 425–435, (1972).

[32] Eringen, A.C., and Edelen, D.G.B., "On Nonlocal Elasticity", International Journal of Engineering Science, Vol. 10, No. 3, pp. 233–248, (1972).

[33] Eringen, A.C., "*Nonlocal Continuum Field Theories*", Springer, New York, (2002).

[34] Shokouhmand, H., Isfahani, A. H. M., and Shirani, E., "Friction and Heat Transfer Coefficient in Micro and Nano Channels with Porous Media for Wide Range of Knudsen Number", International Communication in Heat and Mass Transfer, Vol. 37, pp. 890-894, (2010).

Nomenclature

A Area of the structure
E Young Modulus of Elasticity
G Shear Modulus
I moment of area
k_p Pasternak foundation coefficient
k_1 linear Winkler foundation coefficient
k_3 nonlinearWinkler foundation coefficient
Kn Knudsen number,
l_o, l_1,$l_2$independent length scale parameters
L length
m_p mass of the structure
$m_f$mass of fluid
N axial/Longitudinal force
P Pressure
$r$radius of the structure
t time
T tension
$u(t)$ generalized coordinate of the system
w transverse displacement/deflection
x axial coordinate
$Z_o(x)$ is the arbitrary initial rise function.
σ_v tangential moment accommodation coefficient
$\phi(x)$ trial/comparison function
υPoisson' ratio
μ damping coefficient
$\Delta\theta$ change in temperature
α coefficient of expansion

چکیده

در کار حاضر، حل تحلیلی برای معادلات غیرخطی حاصل از ارتعاشات اجباری ناشی از حرارت و اثر سیال در سازه‌های حامل سیال با استفاده از روش تبدیل دیفرانسیلی گالرکین ارائه شده است. نتایج تحلیل نشان می‌دهند که افزایش طول و نسبت ابعادی سازه حاوی سیال باعث کاهش فرکانسهای غیرخطی سازه می‌گردد. در صورتی که افزایش سرعت سیال باعث افزایش فرکانسهای ارتعاش غیرخطی سازه می‌گردد. همچنین افزایش پارامتر لغزش باعث کاهش در فرکانس طبیعی سازه و سرعت بحرانی سیال می‌شود.

از طرف دیگر افزایش پارامتر لغزش باعث کاهش در نسبت فرکانس بدون بعد سازه می‌شود. با افزایش عدد نادسن، سفتی خمشی نانولوله کاهش پیدا می‌کند و در نتیجه سرعت بحرانی جریان با انتقال منحنی به فرکانس پایین‌تر کاهش پیدا می‌کند. نتایج بدست آمده از روش تبدیل دیفرانسیلی در مقایسه با نتایج حل عددی غیرخطی و حل تحلیل خطی از تطابق خوبی برخوردار است.